Free Radical Biology and Medicine 153 (2020) 34–53

Contents lists available at ScienceDirect

Free Radical Biology and Medicine

journal homepage: www.elsevier.com/locate/freeradbiomed

Original article

The photodynamic and direct actions of methylene blue on mitochondrial energy metabolism: A balance of the useful and harmful effects of this photosensitizer

Eduardo Makiyama Klosowski[a,1], Byanca Thais Lima de Souza[a,1], Marcio Shigueaki Mito[a], Renato Polimeni Constantin[b], Gislaine Cristiane Mantovanelli[a], Juliana Morais Mewes[a], Paulo Francisco Veiga Bizerra[a], Paulo Vinicius Moreira da Costa Menezes[a], Eduardo Hideo Gilglioni[a], Karina Sayuri Utsunomiya[a], Rogério Marchiosi[b], Wanderley Dantas dos Santos[b], Osvaldo Ferrarese Filho[b], Wilker Caetano[c], Paulo Cesar de Souza Pereira[c], Renato Sonchini Gonçalves[c], Jorgete Constantin[a], Emy Luiza Ishii-Iwamoto[a], Rodrigo Polimeni Constantin[a,*]

[a] Department of Biochemistry, Laboratory of Biological Oxidations and Laboratory of Experimental Steatosis, State University of Maringá, Maringá, 87020-900, Paraná, Brazil
[b] Department of Biochemistry, Laboratory of Plant Biochemistry, State University of Maringá, Maringá, 87020-900, Paraná, Brazil
[c] Department of Chemistry, State University of Maringá, Maringá, 87020-900, Paraná, Brazil

ARTICLE INFO

Keywords:
Isolated mitochondria
Photodynamic effect
Mitochondrial energy metabolism
Uncoupling
Liver toxicity

ABSTRACT

According to the literature, methylene blue (MB) is a photosensitizer (PS) with a high affinity for mitochondria. Therefore, several studies have explored this feature to evaluate its photodynamic effects on the mitochondrial apoptotic pathway under normoxic conditions. We are aware only of limited reports regarding MB's photodynamic effects on mitochondrial energy metabolism, especially under hypoxic conditions. Thus, the purposes of this study were to determine the direct and photodynamic acute effects of MB on the energy metabolism of rat liver mitochondria under hypoxic conditions and its direct acute effects on several parameters linked to energy metabolism in the isolated perfused rat liver. MB presented a high affinity for mitochondria, irrespective of photostimulation or proton gradient formation. Upon photostimulation, MB demonstrated high *in vitro* oxidizing species generation ability. Consequently, MB damaged the mitochondrial macromolecules, as could be evidenced by the elevated levels of lipid peroxidation and protein carbonyls. In addition to generating a pro-oxidant environment, MB also led to a deficient antioxidant defence system, as indicated by the reduced glutathione (GSH) depletion. Bioenergetically, MB caused uncoupling of oxidative phosphorylation and led to photodynamic inactivation of complex I, complex II, and F_1F_O–ATP synthase complex, thus decreasing mitochondrial ATP generation. Contrary to what is expected for an ideal PS, MB displayed appreciable dark toxicity on mitochondrial energy metabolism. The results indicated that MB acted via at least three mechanisms: direct damage to the inner mitochondrial membrane; uncoupling of oxidative phosphorylation; and inhibition of electron transfer. Confirming the impairment of mitochondrial energy metabolism, MB also strongly inhibited mitochondrial ATP production. In the perfused rat liver, MB stimulated oxygen consumption, decreased the ATP/ADP ratio, inhibited gluconeogenesis and ureogenesis, and stimulated glycogenolysis, glycolysis, and ammoniagenesis, fully corroborating its uncoupling action in intact cells, as well. It can be concluded that even under hypoxic conditions, MB is a PS with potential for photodynamic effect-induced mitochondrial dysfunction.

* Corresponding author.
E-mail addresses: eduardomk8@hotmail.com (E.M. Klosowski), byathais@hotmail.com (B.T.L. de Souza), m_s_mito@yahoo.com.br (M.S. Mito), rpconstantin@gmail.com (R.P. Constantin), laine_mantovanelli@hotmail.com (G.C. Mantovanelli), juliana.mewes@outlook.com (J.M. Mewes), paulo_veiga22@hotmail.com (P.F.V. Bizerra), pvmcmenezes@hotmail.com (P.V.M.d.C. Menezes), gilglioni@hotmail.com (E.H. Gilglioni), karina.utsunomiya@gmail.com (K.S. Utsunomiya), rmarchiosi@uem.br (R. Marchiosi), wdsantos@uem.br (W.D. dos Santos), oferrarese@uem.br (O.F. Filho), wcaetano@uem.br (W. Caetano), paulocamver@gmail.com (P.C.d.S. Pereira), rsgoncalves2@uem.br (R.S. Gonçalves), jconstantin@uem.br (J. Constantin), eliiwamoto@uem.br (E.L. Ishii-Iwamoto), rpconstantin@uem.br (R.P. Constantin).
[1] Eduardo Makiyama Klosowski and Byanca Thais Lima de Souza contributed equally and should be considered co-first authors.

https://doi.org/10.1016/j.freeradbiomed.2020.04.015
Received 31 January 2020; Received in revised form 13 April 2020; Accepted 13 April 2020
Available online 18 April 2020
0891-5849/ © 2020 Elsevier Inc. All rights reserved.

However, MB disrupts the mitochondrial energy metabolism even in the dark, causing energy-linked liver metabolic changes that could be harmful in specific circumstances.

1. Introduction

Photodynamic therapy (PDT) is a clinical therapeutic procedure for the treatment of neoplastic and non-neoplastic diseases that involves the combination of a photosensitizer (PS), light with the proper wavelength, and molecular oxygen. Ideally, these three elements should be nontoxic separately, but jointly, they should be able to induce the generation of reactive oxygen species (ROS) that can damage cellular constituents, leading to cell death [1,2]. The PDT is, therefore, a two-stage procedure in which the PS is systemically, locally, or topically administrated to the subject, followed by illumination of the target tissue with a specific wavelength light. Since the PS is activated via direct illumination, in general, only the target tissue where the PS has been localized is damaged, minimizing side effects [2].

The photochemical mechanisms associated with the damage of biomolecules such as lipids, proteins, and nucleic acids have been classically defined as Type I and Type II mechanisms. The first class (Type I) involves hydrogen-atom abstraction or electron-transfer reactions between the triplet photoexcited PS and surrounding substrates, such as lipids and proteins. These reactions produce free radicals which react with molecular oxygen to form ROS, such as superoxide anion radicals ($O_2^{\bullet-}$), hydroxyl radicals ($HO^{\bullet}$), and hydrogen peroxide (H_2O_2). Alternatively, in the Type II mechanism, the energy available in the triplet photoexcited PS can be directly transferred to molecular oxygen, leading to the intracellular production of singlet oxygen ($^1O_2$), which is not a free radical but – similarly to other ROS – is capable of damaging biomolecules [3–5]. Although most of the experimental studies suggest that $^1O_2$ is the protagonist in *in vivo* PDT, it is important to note that both Type I and Type II mechanisms can occur simultaneously, leading to comparable oxidative damage [4,5]. The ratio between these routes depends on the nature of the PS and – crucially – on the cellular microenvironment where the PS is accumulated, which includes the concentrations of molecular oxygen and other substrates [4,5].

Methylene blue (MB) is a tricyclic phenothiazinium PS with promising applications in the PDT for anti-neoplastic treatment [6] that embodies many of the features of an ideal PS. Its protonated chemical structure is shown as an inset in Fig. 1. It has low cost and is commercially available. Additionally, it has high purity and stable composition, as well as an adequate hydrophilic/lipophilic balance which allows its transport across cell membranes and facilitates the intracellular uptake. It also has strong absorption with a high extinction coefficient ($\mathcal{E}$) within the range of 600–900 nm, high singlet oxygen quantum yield ($\Phi_\Delta{}^1O_2$) generation (i.e. as a Type II PS), and selectivity for certain tumour cells [3,7–10]. In addition to these features, several studies suggest that MB possesses minimal dark toxicity (i.e. activated only upon irradiation) [3,7–9]. This is corroborated by the fact that besides its applicability in PDT, MB has been used in medical practice with numerous therapeutic purposes, such as in the treatment of methemoglobinemia and malaria, carbon monoxide or cyanide poisoning, ifosfamide encephalopathy, and neurodegenerative diseases [11–14].

At the cellular level, MB can easily cross the cell membrane, being distributed to several subcellular compartments including lysosomes and mitochondria [3,7,12,14]. The affinity of MB for mitochondria seems to have an apparent special connection. According to several studies, due to its hydrophilic/lipophilic nature and the presence of a positive charge, this compound may accumulate in the mitochondria, being driven by the mitochondrial membrane potential ($\Delta\Psi_m$). Once within the mitochondria, MB is largely retained and can interact with nucleic acids, proteins, and lipids – thereby modulating their functions [3,7,12]. In particular, regarding its effects on the mitochondrial energy metabolism, MB can act as either an inducer or a repressor, apparently depending on the experimental circumstances. For instance, in a recent study, Piel and colleagues [15] demonstrated that an MB dose dependently (5–80 μM) increased respiration in human platelets with rotenone-induced complex I inhibition. In this case, the increase in respiration was not caused by increased coupled respiration, but elevated non-coupled and non-mitochondrial respiration [15]. These effects are supported by a more detailed study with isolated rat liver mitochondria [16] that demonstrated an uncoupling effect for MB at concentrations beginning at 0.5 μM. The same study demonstrated that in addition to directly impairing oxidative phosphorylation, MB induces mitochondrial swelling, suggesting that ultrastructural changes may also support the uncoupling effect. However, this specific impairment occurred only at concentrations above 5 μM [16]. Despite the harmful effects that MB apparently can exert on mitochondrial energy metabolism, this compound is best known for its beneficial bioenergetic effects on mitochondria from different cells and animal models [12,17–20]. In general terms, the molecular mechanism of these effects seems to be

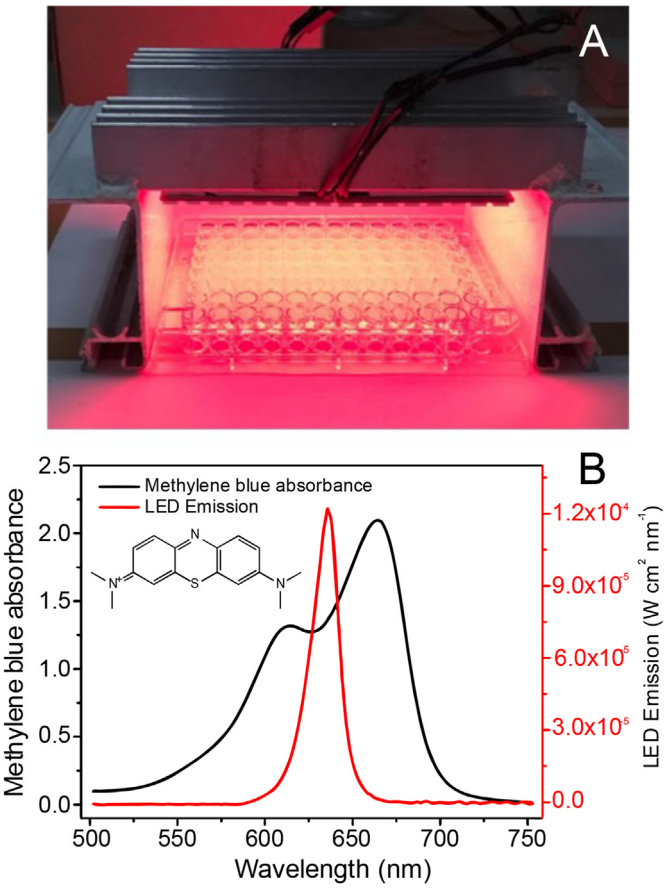

Fig. 1. A) homemade light irradiation emitting source, comprising 192 light emission diodes (LEDs) of the type surface-mounted LED modules (SMD) units with 5 mm diameter, emitting red light with a maximum wavelength at 636 nm (λmáx). B) Overlapping of electronic spectrum of aqueous methylene blue solution ($2{,}2 \times 10^{-5}$ mol L^{-1}; $\varepsilon_{664} = 9.5 \times 10^5$ L mol^{-1} cm^{-1}) and the red-light irradiation emitting source spectrum (surface-mounted LED modules) with absolute irradiance [122×10^{-6} W cm^{-2} nm^{-1}] and integrated irradiance of 2.6 mW cm^{-2}; $\lambda_{emission}$ máx = 636 nm. (For interpretation of the references to colour in this figure legend, the reader is referred to the Web version of this article.)

related to the low MB redox potential of 11 mV. This allows for an effective cycling between the oxidized and reduced forms of MB, which facilitates electron transport in the mitochondria and enhances the ATP production through the oxidative phosphorylation [13,18,21,22]. Most studies claim that this enhancing mitochondrial bioenergetic effect of MB occurs at nM or low μM concentrations (up to 10 μM) [12,18,19,21,22], whereas others suggest that such effects can be achieved even at high μM concentrations (up to 60 μM) [17].

Since MB apparently targets energized mitochondria with a high degree of specificity and alters the energy metabolism of this organelle, as demonstrated by the studies mentioned above, when localized in the mitochondria, if photoactivated using a light with the proper wavelength, MB can also damage the mitochondria [7]. Several photodynamic studies have explored this feature. Most of them, however, are focused only on the influence of MB's photodynamic effects on the general mechanisms of mitochondrial apoptotic pathway (i.e. ROS generation, mitochondrial swelling, and release of mitochondrial apoptotic lethal proteins to the cytosol) or other kind of cell death induction [7,9,23,24]. Less attention has been paid to the molecular mechanisms of MB's photodynamic effects on the parameters of mitochondrial energy metabolism. Moreover, the mitochondrial mechanisms by which MB's photodynamic effects can trigger the mitochondrial apoptotic pathway have been suggested, principally based on studies performed in cell cultures under normoxic conditions (water-saturated atmosphere containing 5% CO_2 and 95% O_2 or air) [9,23]. However, *in vitro* studies performed in normoxic conditions are not ideal for mimicking the hypoxic solid tumour cells' microenvironment and thus poorly reflect the way MB PDT could affect the mitochondrial energy metabolism of tumour cells *in vivo*. Thus, the present study was firstly planned to determine the direct and photodynamic acute effects of MB, in the range of 0.5 to 40 μM, on mitochondrial energy metabolism of isolated mitochondria under an environment that simulates pathological hypoxia (oxygen level of 3.68 mmHg or 190 μM), a condition predominantly found in solid tumours [25]. In this case, the isolated rat liver mitochondria were used as a study model.

As it occurs with most xenobiotics, MB is at least partially biotransformed in the liver [26]. Considering that MB possibly impairs the oxidative phosphorylation by an uncoupling effect when in contact with isolated mitochondria [16], the most expected consequence of an impairment of oxidative phosphorylation is a reduction in the concentration of cellular ATP, as indeed demonstrated in the livers of rats that received liquid diets which contained MB at a concentration of 130 mg/L for 22 days [27]. The same study demonstrated that in this circumstance, MB also decreased the hepatic cytosolic and mitochondrial NADH to NAD^+ ratios of rats who were concomitantly treated with ethanol, indicating that this effect could affect availability of NADH for mitochondrial NADH oxidation and oxidative phosphorylation [27]. This relationship between MB exposure and the liver inevitably leads to the question of whether this compound can also affect specific metabolic pathways that are dependent on ATP and/or NADH. One such process is gluconeogenesis, which is strictly dependent on mitochondrial ATP synthesis and reducing power in the form of NADH. Therefore, another objective of this study was to examine the possible acute direct effects of MB, in the range of 5 to 40 μM, on liver metabolic pathways linked to energy metabolism, particularly gluconeogenesis, glycolysis, glycogenolysis, and ureogenesis. These experiments were performed in the isolated perfused rat liver, an experimental system that permits the measurement of metabolic phenomena under conditions closer to the physiological environment, in which the microcirculation, cell polarity, and cell integrity are preserved [28]. Given the therapeutic potential of MB and its current use in PDT and other medicinal applications, it is highly necessary to more comprehensively characterize its mode of action in biological systems. Thus, the results of the present study should enhance our knowledge of the direct and photodynamic acute modes of action of MB and provide additional information for its possible toxicological effects, as within a certain limit, it is generally recognized as a safe compound.

2. Materials and Methods

2.1. Materials

The PS MB was purchased from Sigma-Aldrich (St. Louis, MO, USA) and recrystallized with ethanol. Substrates, enzymes, and coenzymes were also purchased from Sigma-Aldrich (St. Louis, MO, USA). All other reagents were obtained at the highest available grade.

2.2. Animals

Male Wistar rats weighing 180–220 g and fed *ad libitum* with a standard laboratory diet (Nuvilab CR-1®) were housed in polycarbonate cages in a controlled environment, with a 12:12 h light-dark cycle starting at 06:00 a.m., at 20–23 °C. For all the experiments, the rats were anaesthetized by an intraperitoneal injection of sodium thiopental-lidocaine (50–4 mg/kg) before removal of the liver. In the experimental protocols to evaluate gluconeogenesis, the rats were deprived of food overnight (12 h) before the experiments. The experiments were conducted in the morning (8:00 a.m. to 9:00 a.m.). All experiments were conducted in strict adherence with the guidelines of the Ethics Committee for Animal Experiments of the State University of Maringá (Registered number 2132280318).

2.3. MB's photodynamic action upon mitochondrial metabolism

MB's electronic absorption spectra and fluorescence emission spectra were monitored spectrophotometrically and spectrofluorometrically, respectively. To assess the influence of MB on mitochondrial energy metabolism and related parameters, pre-incubations containing the organelle were performed in the presence of several MB concentrations in the range of 0 μM up to 40 μM. The pre-incubations were kept in the dark or were photoexcited for 10 min under light irradiation with specific energy and controlled photon dosimetry. The mitochondrial-containing pure incubations were also monitored under light photostimulation and considered as controls. Pre-incubations were performed on clear acrylic plates for cell cultures containing 6 wells, with volumes varying between 0.5-2.0 mL. After this step, the respective protocols of each test were performed. In all cases, MB was dissolved in the reaction media without the addition of adjuvants.

For irradiation of pure and MB-loaded mitochondria incubations, a specific homemade light irradiation emitting source was used, comprising 192 light emission diodes (LEDs) of the type surface-mounted LED modules (SMD) units with 5 mm diameter, emitting red light with a maximum wavelength at 636 nm (λmáx) (Fig. 1A). The illumination device has been properly designed in order to fit a suitable setup experimental for *in vitro* studies involving 6 up to 96-well plates, and disposed at 5 cm from the sample surface, providing a homogeneous and thermally stable lighting time for a 10 min period, with an integrated irradiance power of 2.6 mW × cm^2 and therefore providing an overall photon energy dose (fluence) of 1.6 J × cm^{-2}. The optical parameters of the red light SMD-LED source – such as emission spectrum and absolute and integrated irradiance – were measured by a spectroradiometer. As observed in Fig. 1B, there is a reasonable overlap of the emission source and the MB electronic spectra, which present a singlet oxygen quantum yield ($\Phi_\Delta{}^1O_2$) of ~0,5 [7], a fundamental requisite for photodynamic action.

2.4. Mitochondria isolation

The fed rats were anaesthetized, and their livers were removed immediately and cut into small pieces. After homogenization, the mitochondria were isolated by differential centrifugation and kept at 0–4 °C [29,30]. When necessary, mitochondria were disrupted by

successive freezing and thawing procedures using liquid nitrogen. The protein content of the mitochondrial suspensions was measured using the Folin-phenol reagent and bovine serum albumin as standard [31].

2.5. Binding of the MB to the mitochondria

The binding of the MB to the mitochondria was determined as described previously [32]. Two mitochondrial preparations were used: (a) non-energized intact mitochondria; and (b) intact mitochondria energized with a mixture of 10 mM succinate, 10 mM glutamate, and 10 mM malate. After 10 min of incubation under light or in the dark, the mitochondrial suspensions were immediately centrifuged for 5 min at 10,000 × *g* in a refrigerated centrifuge (2 °C). The MB in the supernatant, was measured spectrophotometrically at 630 nm. The compound concentrations in the samples were calculated using the regression parameters obtained from a calibration curve (y = 0.02164x - 0,00712). As denoted by the correlation coefficient closest to unity (0.9996), linear relationships were obtained between the concentrations and the absorbances. The bound MB was calculated by subtraction (added MB – free MB), expressed as nmol/mg protein and discussed in the text in percentage terms (mean binding degrees).

2.6. MB capacity of producing oxidizing species in a mitochondria-free system

An indirect total oxidizing species detection was performed, based on the oxidation of 2′,7′-dichlorodihydrofluorescein diacetate (DCFH-DA) to its green fluorescent form 2′,7′-dichlorofluorescein (DCF) [33]. After hydrolysis of DCFH-DA and pH adjustment (20 mM Tris-HCl, pH 7.4), the resulting solution containing 2′,7′-dichlorodihydrofluorescein (DCFH) was transferred to 6-well plates and incubated in the absence (control) and in the presence of variable MB concentrations (5—40 μM) for 10 min in the dark or under light. The formation of DCF was measured initially and immediately after 10 min of incubation using a spectrofluorometer (504 nm excitation and 529 nm emission). MB interference was excluded by running blanks. Data were expressed as fluorescence intensity in arbitrary units (a.u.), considering the difference between the fluorescence in the initial and final time during the 10 min period.

2.7. Quantification of oxidative injury parameters, protein thiol groups, and reduced glutathione in isolated mitochondria

Disrupted rat liver mitochondria were assayed for oxidative damage parameters and the contents of protein thiol groups and reduced glutathione (GSH). The carbonylated protein content was determined with the use of 2,4-dinitrophenylhydrazine (DNPH), calculated using the molar absorption coefficient for aliphatic hydrazones at 370 nm of 22,000 $M^{-1} \times cm^{-1}$ and expressed as nmol/mg protein [34]. Lipid peroxidation was evaluated using thiobarbituric acid reactive substances (TBARS), predominantly malondialdehyde (MDA). The absorbance was determined at 532 nm ($\varepsilon = 1.56 \times 10^5\ M^{-1}\ cm^{-1}$), the amount of lipoperoxides was calculated from the standard curve prepared with 1,1′,3,3′-tetraethoxypropane, and the values were expressed as nmol/mg protein [35]. The protein thiol (sulfhydryl) contents were determined using the compound 5,5-dithiobis 2-nitrobenzoic acid (DTNB), measured at 412 nm, calculated using a molar extinction coefficient of $1.415 \times 10^4\ M^{-1}\ cm^{-1}$ and expressed as nmol/mg protein [36]. The GSH contents were measured fluorometrically (350 nm excitation and 420 nm emission) using o-phthalaldehyde (OPT). The results were expressed as μg GSH/mg protein in the mitochondrial suspension [37].

2.8. Determination of the respiratory activity of isolated mitochondria

Oxygen consumption by coupled isolated mitochondria was measured polarographically [29,32,38]. The rates of oxygen consumption were expressed as nmol/min × mg protein. The respiratory control ratio (RC) and the ADP/O ratio were calculated as described previously [39]. Freeze-thawing-disrupted mitochondria were used as an enzyme source for assaying membrane-bound enzymatic activities [40,41]. Rates of oxygen consumption were expressed as nmol/min × mg protein. Considering that MB presents the ability to non-enzymatically oxidize NADH [42] with concomitant oxygen consumption [43], when the effects of MB on NADH oxidase were assessed, such interference was excluded through the execution of blanks.

2.9. ATPase activity

The mitochondrial ATPase activity was assayed by measuring the phosphate release [41,44,45] and the wavelength was set at 780 nm instead of 700 nm to avoid MB interference. The results were expressed as nmol of phosphate released/min × mg protein.

2.10. Determination of mitochondrial ATP production

Intact mitochondria (3.3 mg protein/mL) were incubated at 37 °C in the same reaction medium used for oxygen measurements [29,46] and containing an additional 10 mM succinate plus 5 μM rotenone or 10 mM malate plus 10 mM glutamate. The reaction was initiated by the addition of 1.0 mM ADP and stopped after 20 min by the addition of 0.6 M perchloric acid. After centrifugation at 4,000 × *g* for 10 min (2 °C), the supernatant was neutralized with K_2CO_3, and the potassium perchlorate was removed by centrifugation at 4,000 × *g* for 5 min (2 °C). The supernatant was assayed for ATP content using high-performance liquid chromatography (HPLC) [41,47].

2.11. Succinate-dehydrogenase activity

The succinate-dehydrogenase activity was assayed at 420 nm using ferricyanide as electron acceptor [40]. The results were expressed as nmol ferricyanide reduced/min × mg protein.

2.12. Mitochondrial swelling

The swelling driven by the oxidation of organic substrates and ATP hydrolysis was followed spectrophotometrically at 520 nm [48]. The reactions were initiated by the concomitant addition of sodium acetate (50 mM) and the following substrates: a) 10 mM succinate; b) 10 mM glutamate; c) 0.2 mM TMPD with 5 mM ascorbate; and d) 2 mM ATP. The maximal amplitude of absorbance and the rate of absorbance decrease were expressed as fractions of corresponding controls and plotted versus the MB concentrations.

2.13. Inner mitochondrial membrane integrity

The inner mitochondrial membrane integrity was assessed as previously described [47]. The decrease in absorbance at 340 nm, due to oxidation of NADH (0.08 mM), was recorded spectrophotometrically. The results were expressed as nmol NADH oxidized/min. Considering that MB presents the ability to non-enzymatically oxidize NADH [42] with concomitant oxygen consumption [43], when the effects of MB on inner mitochondrial membrane integrity were assessed, such interference was excluded through the execution of blanks.

2.14. Measurement of NADH and GSH oxidation in a mitochondria-free system

The action of MB on NADH oxidation was measured as described previously [42]. The preincubation reaction medium contained 20 mM Tris-HCl (pH 7.4) and different MB concentrations (0.5—40 μM). After the 10-min preincubation, the content was transferred to a cuvette, and

0.4 mM NADH was added to start the reaction. The oxidation of NADH was monitored at 340 nm using a spectrophotometer. The results were expressed as nmol NADH oxidized/min. The oxygen consumption from this reaction was measured polarographically [38], and expressed as nmol oxygen consumed/min.

The action of MB on GSH oxidation was measured as described previously [49]. The reaction medium contained 50 mM potassium phosphate buffer (pH 7.4), 1 mM EDTA, 0.05 mM GSH, and different MB concentrations (0.5—40 μM). After the 10-min preincubation, the reaction was started by adding 0.5 mM DTNB. After 15 min of incubation in the dark, the absorbance was determined at 412 nm (ε = 14,150 $M^{-1} \times cm^{-1}$), and the results were expressed as nmol GSH oxidized/min. MB interference (with absorbance at 412 nm) was excluded by running blanks.

2.15. Liver perfusion

The hepatic perfusion experiments were performed only in the absence of photostimulation. The hemoglobin-free, non-recirculating perfusion was performed according to the technique previously described [28,30,32,41]. The following metabolites were quantified by means of standard enzymatic procedures: glucose; pyruvate; lactate; ammonia; and urea [50,51]. Interference by MB (absorbance at 365, 505, and 540 nm) was excluded by running blanks. When necessary, the interference regarding the non-enzymatic reaction between MB and NADH was also excluded by running blanks. The oxygen concentration in the outflowing perfusate was monitored polarographically [38]. The hepatic contents of the adenine nucleotides (ATP, ADP and AMP) were assayed by means of HPLC [41].

2.16. Microsomal oxygen consumption

Microsomes from the livers of fed rats were isolated by differential centrifugation [52]. The oxygen uptake was measured polarographically [38,53,54]. Oxygen uptake was started by adding 0.1 mM NADPH, followed by the addition of different MB concentrations (1—40 μM). Oxygen uptake rates were expressed as nmol/min × mg protein. Considering that MB has the ability to non-enzymatically oxidize NADPH [42] with concomitant oxygen consumption [43], when the effects of MB on microsomal oxygen consumption were assessed, such interference was excluded through the execution of blanks.

2.17. Treatment of data

The statistical significance of differences between the experimental parameters was evaluated by a Student's *t*-test or by Dunnett's multiple comparison test after submitting the data to variance analysis according to its context ($p < 0.05$). Statistical analysis, linear regressions, and half-maximal effect concentrations were obtained using GraphPad Software (San Diego, CA).

3. Results

3.1. Binding degree of MB to isolated rat liver mitochondria

The binding of MB to non-energized (Fig. 2A) and energized (Fig. 2B) mitochondria was observed in both conditions (with and without light). In all cases, the concentration dependence of binding showed a linear relationship, indicating that saturation was not attained in the concentration range up to 40 μM. When non-energized mitochondria were evaluated without light, the mean binding degree (34.0 ± 5.8%) was not statistically different from that assessed under light (40.0 ± 4.8%). When mitochondria previously energized with a mixture of succinate, malate, and glutamate were assessed, the mean binding degree measured without light (45.5 ± 6.8%) was also not statistically different from that assessed under light (36.0 ± 5.8%). Contrary to what was expected, the energization of mitochondria did not enhance the mean binding degree of MB.

3.2. The direct and photodynamic MB capacity of producing oxidizing species in a mitochondria-free system

The ROS generation by MB in a mitochondria-free system was evaluated by using a DCFH-DA assay (Fig. 3A). The incubation mediums were exposed to increasing concentrations of MB for 10 min without light exposure. In the absence of MB (controls), there was no green fluorescence. On the contrary, significant fluorescence was observed in the presence of 20 μM and 40 μM MB. After exposure to light for 10 min, the controls (without MB) still showed no fluorescence, but strong fluorescence was observed in the presence of 20 μM and 40 μM MB (Fig. 3A). The oxidizing species generation under light exposure was 142.2% and 206.3% higher than that in the absence of light at 20 μM and 40 μM MB, respectively.

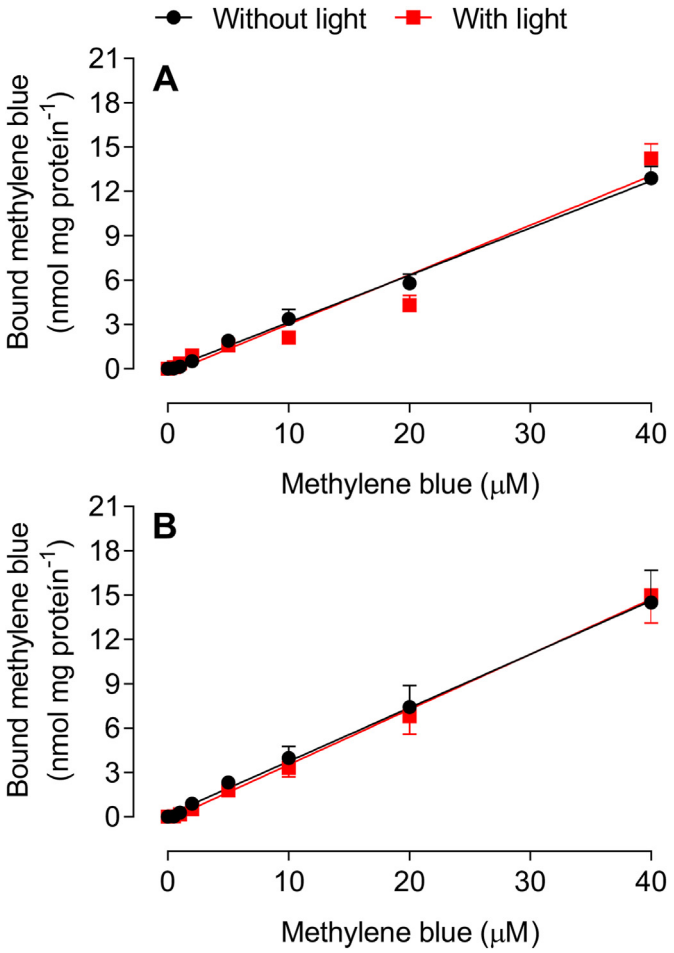

Fig. 2. Binding of methylene blue to isolated rat liver mitochondria. Binding was measured under light or in the dark (non-illuminated) as described in the Materials and Methods section. Each datum point represents the mean of 8 independent experiments. Bars are standard errors of the mean. The continuous lines represent the optimized linear regression curve. A) non-energized intact mitochondria [(linear regression curve without light; y = 0,3189x - 0,0528. R^2 = 0,9961); (linear regression curve with light; y = 0,3347x - 0,3362. R^2 = 0,9555)]. B) Energized intact mitochondria [(linear regression curve without light; y = 0,3624x + 0,1210. R^2 = 0,9980); (linear regression curve with light; y = 0,3736x - 0,2162. R^2 = 0.9979). (For interpretation of the references to colour in this figure legend, the reader is referred to the Web version of this article.)

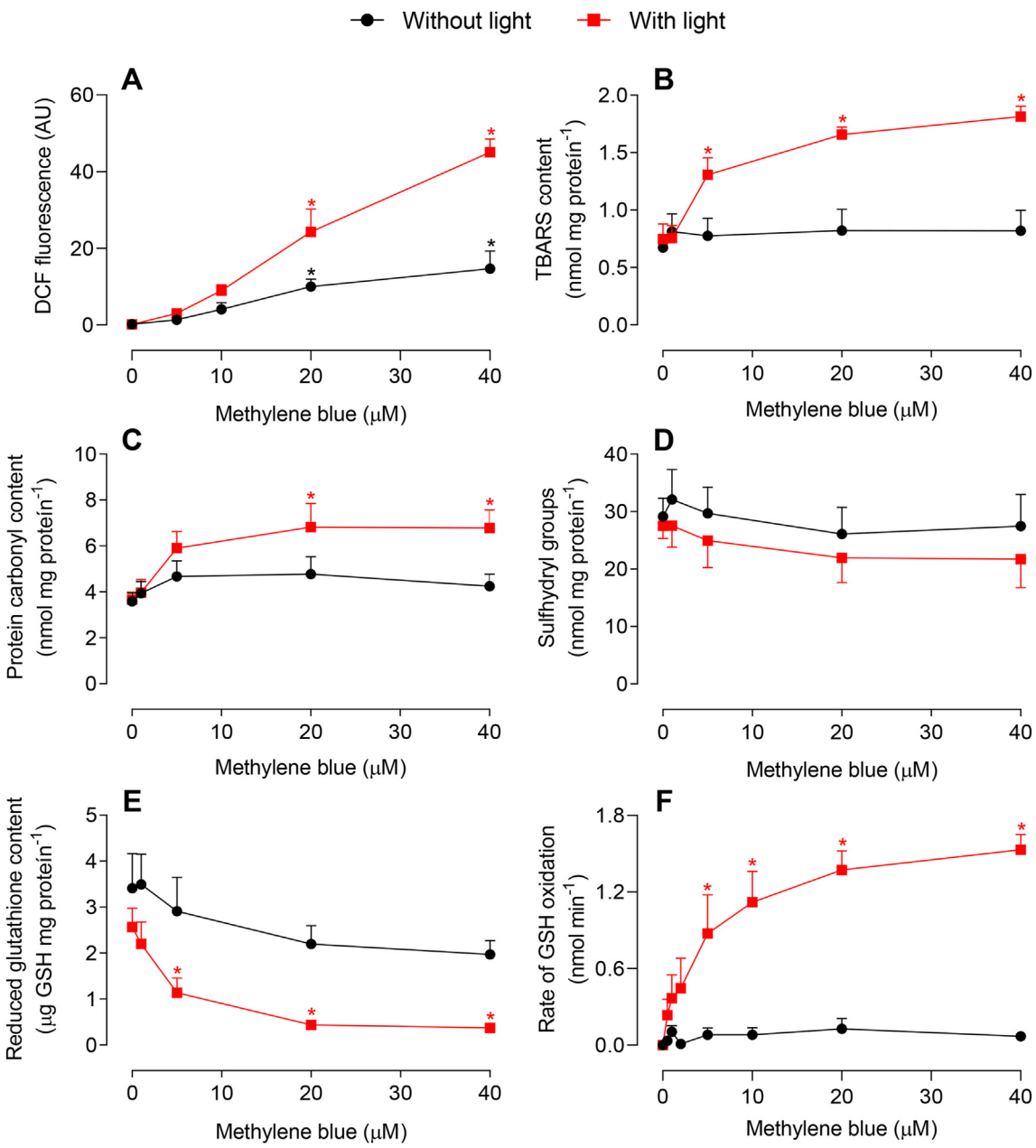

Fig. 3. The effects of methylene blue (with and without light irradiation) on the production of ROS in a mitochondria-free system (A), TBARS (B), carbonylated proteins (C), protein thiol (D) and reduced glutathione (GSH) (E) contents in freeze–thaw-disrupted mitochondria, and the dependence of the rate of GSH oxidation on the methylene blue (with and without light irradiation) concentration (F). Each assay point represents the mean of 3–10 independent experiments and the bars are the standard errors of the mean. *$p < 0.05$, ANOVA with post hoc Dunnett's test. (For interpretation of the references to colour in this figure legend, the reader is referred to the Web version of this article.)

3.3. The direct and photodynamic effects of MB on mitochondrial levels of TBARS, protein carbonyl groups, reduced glutathione, and sulfhydryl protein groups

In the presence of MB, no significant difference in the TBARS levels was found in isolated mitochondria when the measurements were conducted without light. Under light influence, TBARS contents were increased, reaching a 143.0% higher level in the presence of 40 μM MB (Fig. 3B). In line with the results of the TBARS contents, in the presence of MB, no significant difference in the protein carbonyl contents was found when the measurements were conducted without light. Under the light effect, MB at the concentrations of 20 μM and 40 μM significantly increased the protein carbonyl contents by approximately 85% (Fig. 3C). The MB caused no significant difference in the protein thiol content neither without nor with light (Fig. 3D). The addition of MB did not significantly decrease the mitochondrial GSH content in the absence of light. Under the influence of light, GSH contents were significantly decreased, reaching an 85.3% lower level in the presence of 40 μM MB (Fig. 3E).

3.4. The direct and photodynamic effects of MB on GSH oxidation in a mitochondria-free system

The rate of GSH oxidation was represented against different MB concentrations. In a mitochondria-free system and in the absence of light, MB did not promote GSH oxidation. Under the influence of light, however, MB (5—40 μM) was able to cause a significant oxidation of GSH (Fig. 3F).

3.5. The direct and photodynamic effects of MB on parameters of energy transduction in isolated mitochondria

The direct and photodynamic effects of MB on several parameters of energy transduction were evaluated in isolated mitochondria (Fig. 4A–F and Table 1). Irrespective of the substrates that were used in the assays, the action of MB without light on mitochondrial respiration was characterized by a reduction in energy transduction as revealed by inhibition of state III respiration. Inhibition was greater with the substrate succinate (63.1% at 40 μM) when compared to glutamate plus malate (46.2% at 40 μM). Before ADP addition (substrate respiration) and after exhaustion of ADP (state IV respiration), MB increased oxygen consumption with all substrates used in the assays. It is important to note that specifically in the presence of succinate, these parameters were increased by MB with a maximum approximately in the range between 2 μM and 10 μM, whereas an inhibitory tendency took place when the concentration was increased to higher values. The RC ratio was progressively decreased by increasing concentrations of MB with all

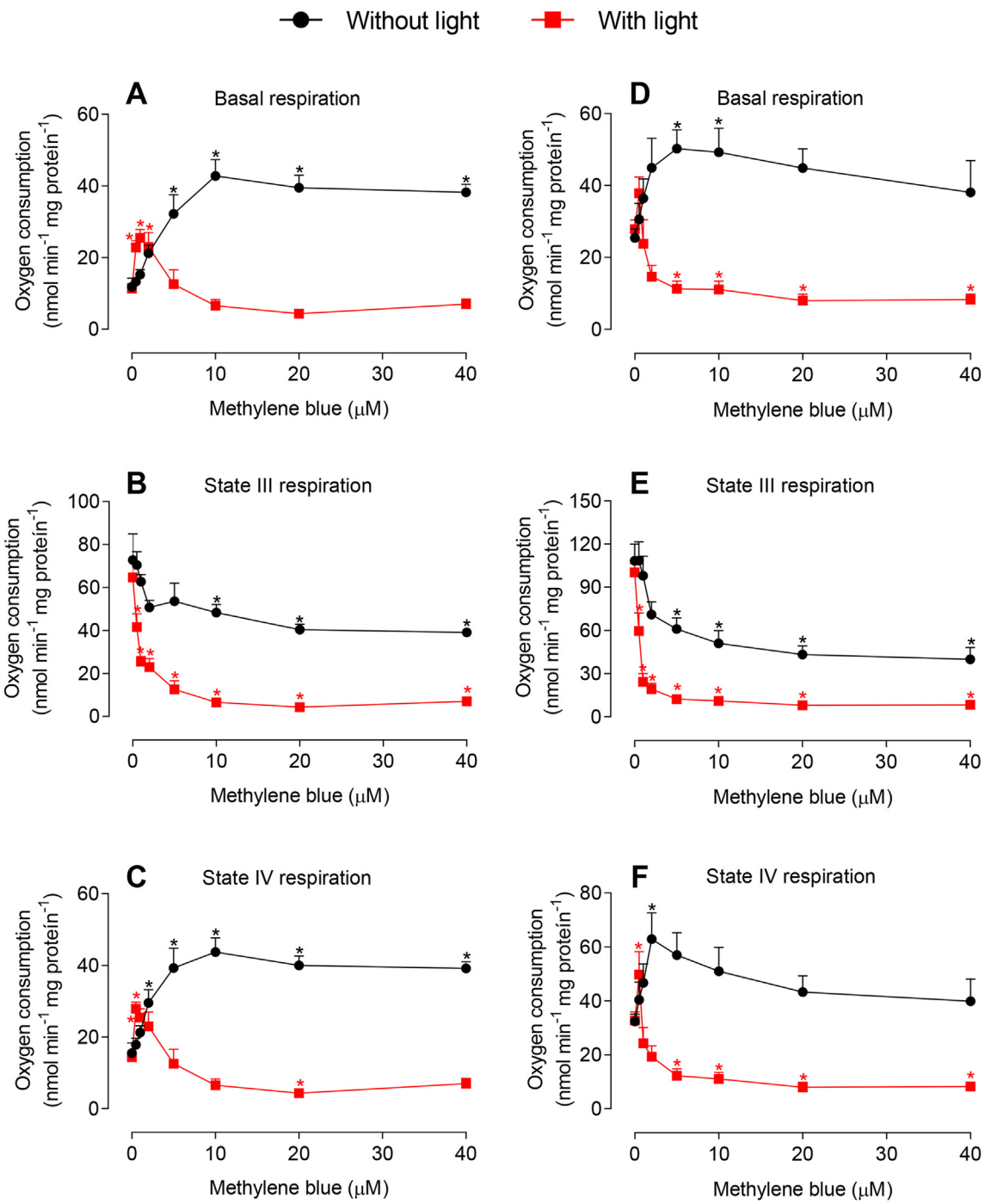

Fig. 4. The effects of methylene blue (with and without light irradiation) on mitochondrial respiration driven by a mixture of malate plus glutamate (A, B and C) and succinate (D, E and F) in the presence or absence of exogenously added ADP. Mitochondria were isolated and assayed as described in the Materials and Methods section. Rates of oxygen consumption were computed from the slopes of the polarographic records. Each datum point represents the mean of 7 independent experiments and the bars are the standard errors of the mean. *$p < 0.05$, ANOVA with post hoc Dunnett's test. (For interpretation of the references to colour in this figure legend, the reader is referred to the Web version of this article.)

Table 1
The effects of methylene blue (with and without light irradiation) on mitochondrial respiration driven by glutamate plus malate and succinate in the presence and absence of exogenously added ADP. Mitochondria were isolated and assayed as described in the Materials and Methods section. Incubations were performed in the presence of the substrates glutamate plus malate and succinate, as indicated. The respiratory control ratio (RC) and the ADP/O ratio were calculated according to the method described by Chance and Williams (1956).

Substrate	Methylene blue (μM)	W ithout light		With light	
		Respiratory control ratio	ADP/O ratio	Respiratory control ratio	ADP/O ratio
Glutamate/ Malate	0	4.92 ± 0.38	2.99 ± 0.36	4.69 ± 0.45	3.06 ± 0.34
	0.5	4.15 ± 0.45	2.90 ± 0.29	1.53 ± 0.24*	1.11 ± 0.56*
	1	3.15 ± 0.40*	2.60 ± 0.18	1.00 ± 0.00*	–#
	2	1.99 ± 0.44*	2.42 ± 0.30	1.00 ± 0.00*	–#
	5	1.45 ± 0.24*	0.92 ± 0.37*	1.00 ± 0.00*	–#
	10	1.14 ± 0.11*	0.56 ± 0.36*	1.00 ± 0.00*	–#
	20	1.01 ± 0.01*	0.35 ± 0.35*	1.00 ± 0.00*	–#
	40	1.00 ± 0.00*	–#	1.00 ± 0.00*	–#
Succinate	0	3.38 ± 0.28	2.13 ± 0.26	3.18 ± 0.23	1.88 ± 0.31
	0.5	2.81 ± 0.19	1.92 ± 0.23	1.17 ± 0.09*	0.69 ± 0.34*
	1	2.17 ± 0.25*	1.41 ± 0.15	1.00 ± 0.00*	–#
	2	1.17 ± 0.11*	0.35 ± 0.23*	1.00 ± 0.00*	–#
	5	1.09 ± 0.07*	0.56 ± 0.39*	1.00 ± 0.00*	–#
	10	1.00 ± 0.00*	–#	1.00 ± 0.00*	–#
	20	1.00 ± 0.00*	–#	1.00 ± 0.00*	–#
	40	1.00 ± 0.00*	–#	1.00 ± 0.00*	–#

Data are the mean ± standard errors of 7 independent experiments with identical protocol. Statistical significance relative to the controls is indicated by asterisks.
*$p < 0.05$, ANOVA with post hoc Dunnett's test.
#No accurate determination possible.

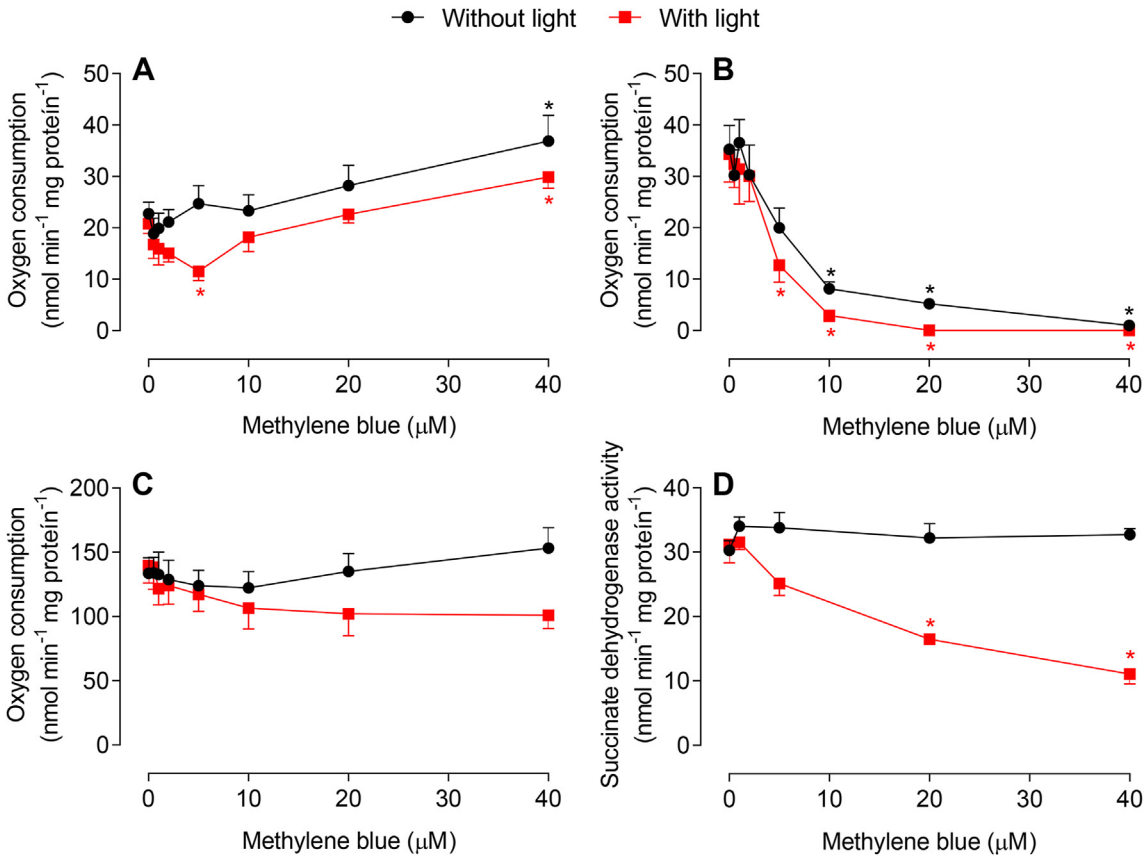

Fig. 5. The effects of methylene blue (with and without light irradiation) on several membrane-bound enzymatic activities in rat liver mitochondria. NADH-oxidase (A), succinate-oxidase (B), TMPD-ascorbate oxidation (C) and succinate dehydrogenase (D) were measured in freeze-thaw-disrupted mitochondria that were incubated at 37 °C in reaction medium as described in the Materials and Methods section. Each datum point represents the mean of 4–6 independent experiments and the bars are the standard errors of the mean. *$p < 0.05$, ANOVA with post hoc Dunnett's test. (For interpretation of the references to colour in this figure legend, the reader is referred to the Web version of this article.)

substrates (Table 1). With succinate as the substrate, for example, no respiratory control at all was found at the MB concentration of 10 μM. Table 1 also shows that MB diminished the ADP/O ratio irrespective of the substrates that were used in the assays. With succinate as the substrate, this reduction was already significant at the concentration of 2 μM MB. Under some circumstances, the ADP/O ratios could not be determined using traditional methods.

Under the influence of light, MB caused an impairment of the mitochondrial energy transduction to a much greater extent than in the absence of light. The inhibition of state III respiration was initiated at the lower concentration of 0.5 μM MB, irrespective of the substrates that were used in the assays. The degree of inhibition of state III respiration reached a maximum of 93.3% and 92.0% in the presence of malate plus glutamate and succinate, respectively. In general terms, substrate respiration and state IV respiration tended to be, or were, stimulated at low MB concentrations with all substrates. However, when the concentration of MB was raised, these parameters tended to be, or were, inhibited. In addition, MB clearly decreased the ADP/O ratios and the RC ratios in both experimental series under the influence of light (Table 1). Complete abolition of respiratory control was found as early as at 1 μM MB, independent of the substrate that was used. The ADP/O ratio was also reduced at 0.5 μM MB and at higher concentrations this parameter could no longer be determined.

3.6. The direct and photodynamic effects of MB on membrane-bound mitochondrial enzymatic activities

The NADH oxidase activity in freeze-thawing disrupted mitochondria was stimulated by MB, but the effect was significant only at the concentration of 40 μM (62.0%). On the contrary, the succinate oxidase activity was almost completely inhibited (97.2%) in the presence of 40 μM MB. MB did not affect the respiration driven by TMPD with ascorbate that reduces the cytochrome c-oxidase. Under light influence, the NADH oxidase activity was inhibited by low MB concentrations, but the effect was significant only at the concentration of 5 μM (44.6%). Stimulation of respiration occurred, on the other hand, in the passage from 5 μM to 10 μM. A significant increment (43.4%) was reached only at 40 μM MB. In absolute terms, the values representing NADH oxidase activity under the influence of light were always smaller than those obtained without light influence at the same MB concentrations. The succinate oxidase activity was strongly inhibited, so that at 20 μM MB, respiration was already completely abolished. The respiration driven by TMPD with ascorbate was not significantly affected by MB even when the measurements were conducted under the influence of light (Fig. 5A–C). Surprisingly, without the influence of light, MB up to 40 μM did not affect succinate dehydrogenase activity. Under light stimulus, however, the succinate dehydrogenase activity was inhibited by 47.1% (20 μM MB) and 64.6% (40 μM MB) (Fig. 5D).

3.7. The direct and photodynamic effects of MB on the catalytic oxidation of NADH in a mitochondria-free system

MB was able to promote significant oxidation of NADH in a mitochondria-free system even when low concentrations were used, with and without the influence of light (Fig. 6A). With high MB concentrations, the rates of NADH oxidation without the influence of light were higher than those obtained under the influence of light. The catalytic oxidation of NADH did indeed occur concomitantly with oxygen consumption (Fig. 6B). Under all experimental conditions, MB stimulated the oxygen consumption in a dose-dependent manner, but a significant definition of this stimulatory effect began only at the concentration of 10 μM. Aligned with the experiments performed spectrophotometrically, with high MB concentrations, the rates of oxygen consumption without the influence of light were higher than those obtained under the influence of light.

3.8. The direct and photodynamic effects of MB on ATPase activity

Fig. 7 (A-C) shows that without photostimulation, MB stimulated the ATPase activity of intact-coupled mitochondria in a saturable way within the concentration range of 5–40 μM. At 40 μM, 369.6% stimulation was found. The ATPase activity of disrupted and uncoupled mitochondria was relatively insensitive to MB within the same concentration range. Under photostimulation the ATPase activity of intact-coupled mitochondria tended to be stimulated by MB in the range up to 5 μM and inhibited at higher concentrations, such that statistical significance was not achieved. The ATPase activity of disrupted and uncoupled mitochondria, however, was strongly inhibited by MB. At 40 μM, ATPase activity was inhibited 93.5% and 92.7% in disrupted and uncoupled mitochondria, respectively.

3.9. The direct effects of MB on mitochondrial swelling

The mitochondrial volume alterations dependent on the energy produced by substrate oxidation or by ATP hydrolysis were determined only without light influence (Fig. 8A–D). MB inhibited the initial rate of the decreases in absorbance and the maximal changes in absorbance

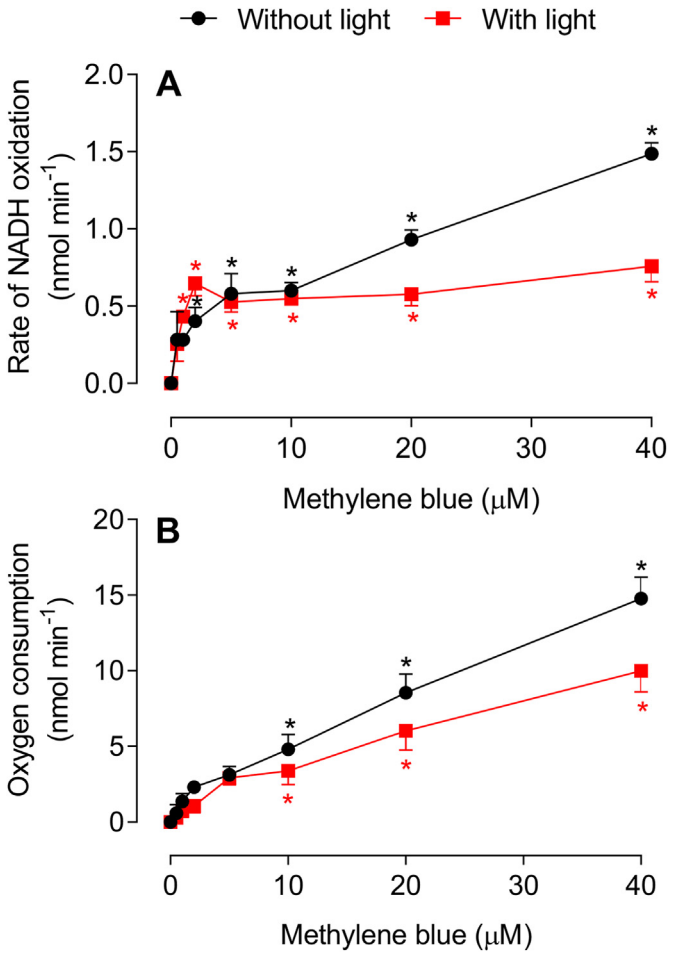

Fig. 6. The dependence of the rate of NADH oxidation (A) and oxygen consumption (B) on the methylene blue concentration (with and without light irradiation). The rate of NADH oxidation was determined at 340 nm in a reaction mixture containing 20 mM Tris-HCl (pH 7.4) and different MB concentrations (0.5—40 μM). The oxygen consumption from this reaction was measured polarographically using a Teflon-shielded platinum electrode. Each datum point represents the mean of 3 independent experiments and the bars are the standard errors of the mean. *$p < 0.05$, ANOVA with post hoc Dunnett's test. (For interpretation of the references to colour in this figure legend, the reader is referred to the Web version of this article.)

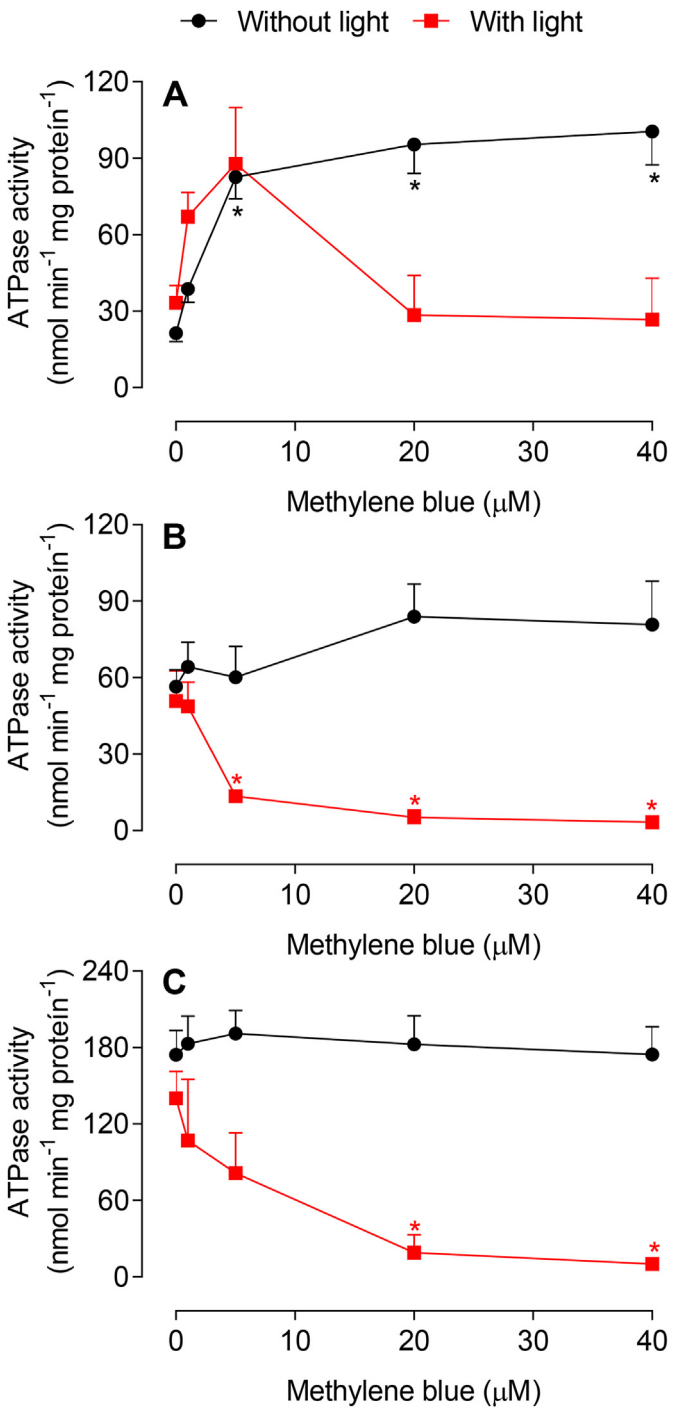

Fig. 7. The effects of methylene blue (with and without light irradiation) on the ATPase activity of coupled (A), disrupted (B) and uncoupled (C) mitochondria. The mitochondria were incubated at 37 °C in reaction medium as described in the Materials and Methods section. Each datum point represents the mean of 5 independent experiments and the bars are the standard errors of the mean. *$p < 0.05$, ANOVA with post hoc Dunnett's test. (For interpretation of the references to colour in this figure legend, the reader is referred to the Web version of this article.)

(amplitude of swelling), independently of the substrate used. The inhibitions were more pronounced when glutamate and succinate were the substrates when compared with ATP or TMPD-ascorbate as the substrates. At 40 μM MB, the inhibition of the initial rate of the decreases reached a maximum of 83.9%, 78.1%, 59.2%, and 60.6% in the presence of glutamate, succinate, TMPD-ascorbate, and ATP, respectively. At the same MB concentration, the decreases in swelling amplitude reached a maximum of 82.3%, 50.5%, and 66.2% in the presence of glutamate, TMPD-ascorbate, and ATP, respectively. When succinate was the substrate, the largest decrease in swelling amplitude was 87.9% at a concentration of 20 μM MB.

3.10. The direct and photodynamic effects of MB on inner mitochondrial membrane integrity

The inner mitochondrial membrane is impermeable to NADH, permitting inner membrane integrity to be evaluated from the increase in the rate of NADH oxidation. In general terms, MB dose dependently stimulated the NADH oxidation with and without light influence. Comparatively, at 40 μM MB, the stimulus reached a maximum of 187.6% and 339.1% with and without light influence, respectively. If one looks at the absolute values of the rates of NADH oxidation, especially at high MB concentrations, it is clear that the maximal values without the influence of light are higher than those the influence of light (Fig. 8E).

3.11. The direct and photodynamic effects of MB on ATP synthesis by oxidative phosphorylation

The addition of MB with and without photostimulation caused inhibition of mitochondrial ATP synthesis independently of the substrates used (Fig. 9A and B). As noted, MB significantly reduced the ATP synthesis as early as the concentration of 5 μM. At this concentration, when glutamate and malate were used as the oxidizable substrates, the inhibition reached a maximum of 92.0% and 47.0% with and without the influence of light, respectively. Similarly, with succinate as the substrate, the ATP synthesis was inhibited by 93.2% and 44.7% with and without the influence of light, respectively.

3.12. The direct effects of MB on gluconeogenesis from lactate and pyruvate

When a mixture of 2.0 mM lactate with 0.2 mM pyruvate was infused in the perfused liver (Fig. 10A), there were extensive increases in both glucose production and oxygen consumption. The infusion of 40 μM MB at 30 min perfusion time caused a fast and substantial decrease in glucose production, with a simultaneous increase in oxygen consumption. When MB infusion was halted at 50 min of perfusion, the glucose production and oxygen consumption tended to recover, but this recovery was still incomplete at the end of the perfusion. Fig. 10B allows an evaluation of several MB concentration effects on oxygen consumption and gluconeogenesis in the range of 5–40 μM. To determine these effects, the rates in the presence of lactate, pyruvate, and MB were subtracted from the rates in the presence of lactate and pyruvate alone. Gluconeogenesis inhibition showed an evident concentration dependence. Half-maximal inhibition can be expected at the MB concentration of 20.2 μM, as revealed by numerical interpolation. Oxygen consumption stimulation showed saturation, as significant increases occurred only at the MB concentrations of 5 μM, 10 μM, and 40 μM. The degree of stimulation reached a maximum of 11.0% at 40 μM MB.

3.13. The direct effects of MB on the adenine nucleotide contents of perfused livers

The contents of ATP, ADP, and AMP were measured in livers from rats submitted to the same conditions as the experiments performed in the fasted condition, in which gluconeogenesis was measured with 2.0 mM lactate and 0.2 mM pyruvate as substrates. The measurements were made in control livers (without MB) and in livers perfused with 40 μM MB (Table 2). The content of ADP was increased (48.0%) by MB when compared with the control values. Consequently, there was a significant diminution (38.8%) in the ratio of ATP/ADP. The ATP and

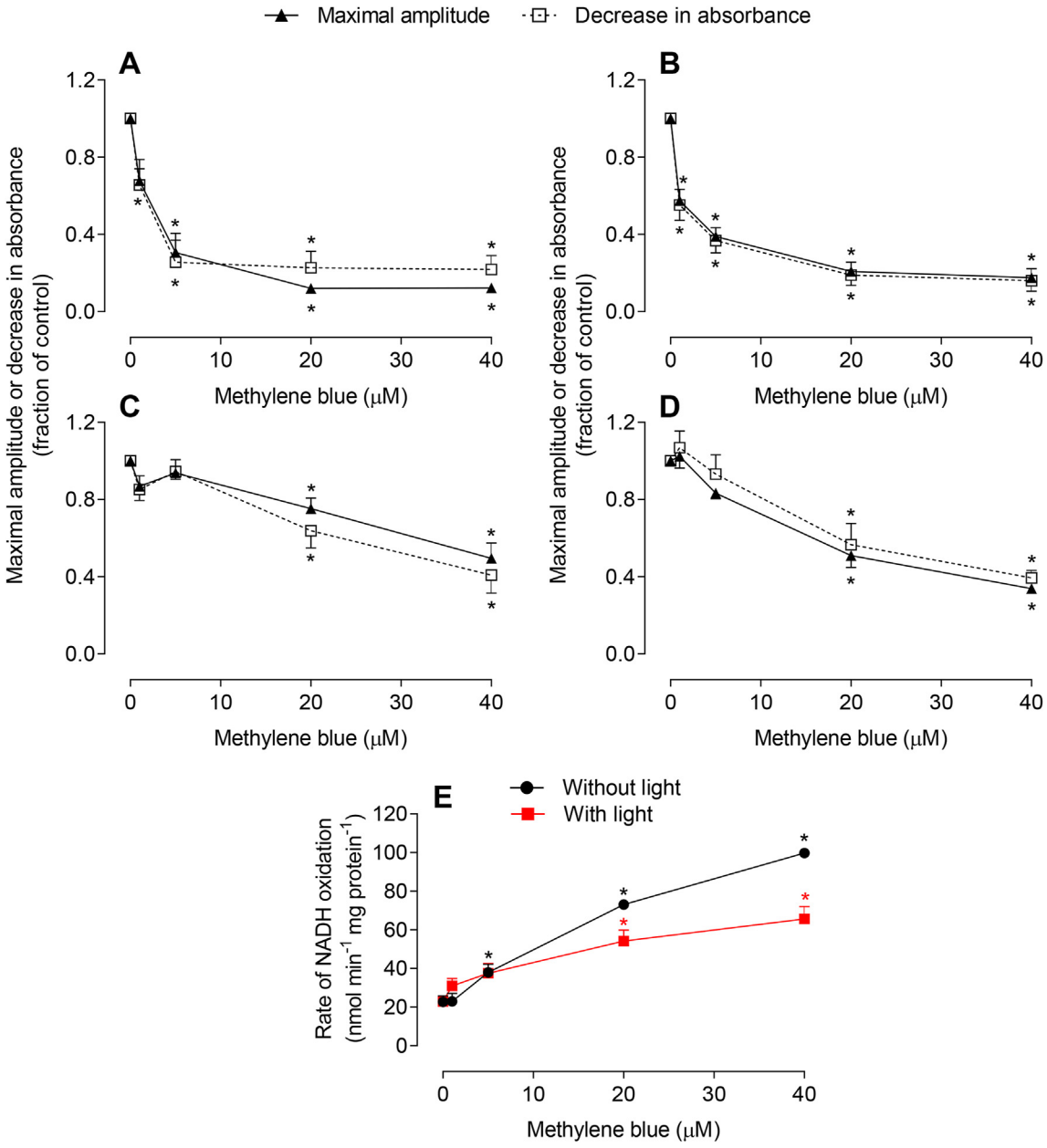

Fig. 8. The effects of methylene blue (without light irradiation) on mitochondrial swelling (A, B, C and D) and the effects of methylene blue (with and without light irradiation) on inner mitochondrial membrane integrity (E). The swelling reactions were initiated by the concomitant addition of sodium acetate (50 mM) and the following substrates: A) 10 mM succinate; B) 10 mM glutamate; C) 0.2 mM TMPD with 5 mM ascorbate; and D) 2 mM ATP. The decrease in absorbance at 520 nm was recorded. The maximal amplitude of absorbance and the rate of absorbance decrease were expressed as fractions of corresponding controls and plotted versus the MB concentrations. The inner mitochondrial membrane integrity (E) was assessed from the increment in the rate of NADH oxidation at 340 nm. Each datum point represents the mean of 3–6 independent experiments and the bars are the standard errors of the mean. *$p < 0.05$, ANOVA with post hoc Dunnett's test. (For interpretation of the references to colour in this figure legend, the reader is referred to the Web version of this article.)

AMP contents, as well as the total amounts of nucleotides (AMP + ADP + ATP) and the ATP/AMP ratio, were not significantly modified.

3.14. The direct effects of MB on gluconeogenesis and ureogenesis from alanine

The infusion of 2.5 mM alanine caused increases in all measured parameters (Fig. 11A and B) which reached steady-state conditions after approximately 15 min. In the presence of 40 μM MB, glucose production was strongly inhibited so that the maximum inhibition (nearly 60%) occurred at 14 min of MB infusion. Oxygen consumption was rapidly stimulated, with a peak value (31.3%) at 6 min of MB infusion. The introduction of MB caused pyruvate production to progressively increase, becoming statistically significant only at 14 min of MB infusion, where the increment reached 65.2%. Lactate production, in turn, was also increased, being statistically significant only at the end of the MB perfusion period (121.1%). Finally, urea production was reduced concomitantly with the increase of ammonia production. The degree of inhibition of urea production reached a maximum of 57.5% after 20 min of MB infusion, and, in the case of ammonia production, the maximum increase (299.0%) occurred after 18 min of MB infusion.

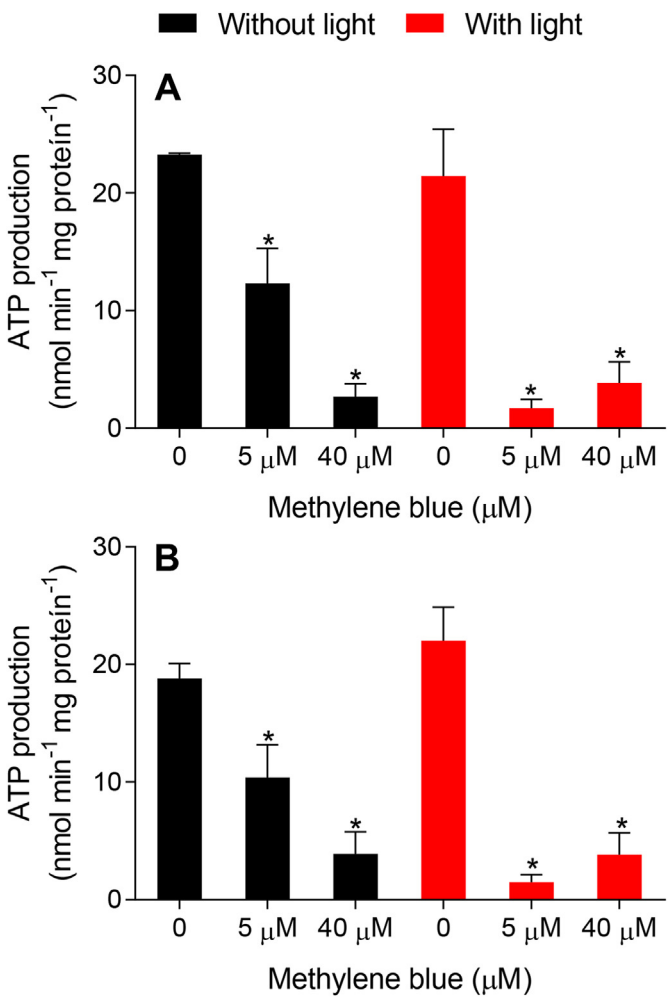

Fig. 9. The effects of methylene blue (with and without light irradiation) on ATP synthesis by mitochondria isolated from rat liver. Mitochondria were incubated as described in the Materials and Methods section in reaction medium containing 10 mM glutamate plus 10 mM malate (A) or 10 mM succinate plus 5 μM rotenone (B). The reaction was initiated by the addition of 1.0 mM ADP and stopped after 20 min by the addition of 0.6 M perchloric acid. The content of ATP in the neutralized extract was determined using high-performance liquid chromatography (HPLC). Each datum point represents the mean of 3–4 independent experiments and the bars are the standard errors of the mean. *$p < 0.05$, ANOVA with post hoc Dunnett's test. (For interpretation of the references to colour in this figure legend, the reader is referred to the Web version of this article.)

3.15. The direct effects of MB on glycogenolysis and glycolysis from endogenous glycogen

As revealed in Fig. 12, all parameters were stable before the beginning of MB infusion. Upon the infusion of 40 μM MB, the oxygen consumption increased and remained so during the entire infusion period. The maximum stimulation (nearly 22%) occurred at 10 min of MB infusion. There was a minor tendency for increased glucose release in the presence of MB, but this lacked statistical significance. Cessation of MB infusion was followed by a decrease in glucose release, with significant inhibition (33.0%) occurring at the end of perfusion time. Finally, 40 μM MB strongly stimulated lactate and pyruvate productions, with peak increments of 92.2% for lactate and 63.3% for pyruvate at 10 min and 14 min of MB infusion, respectively.

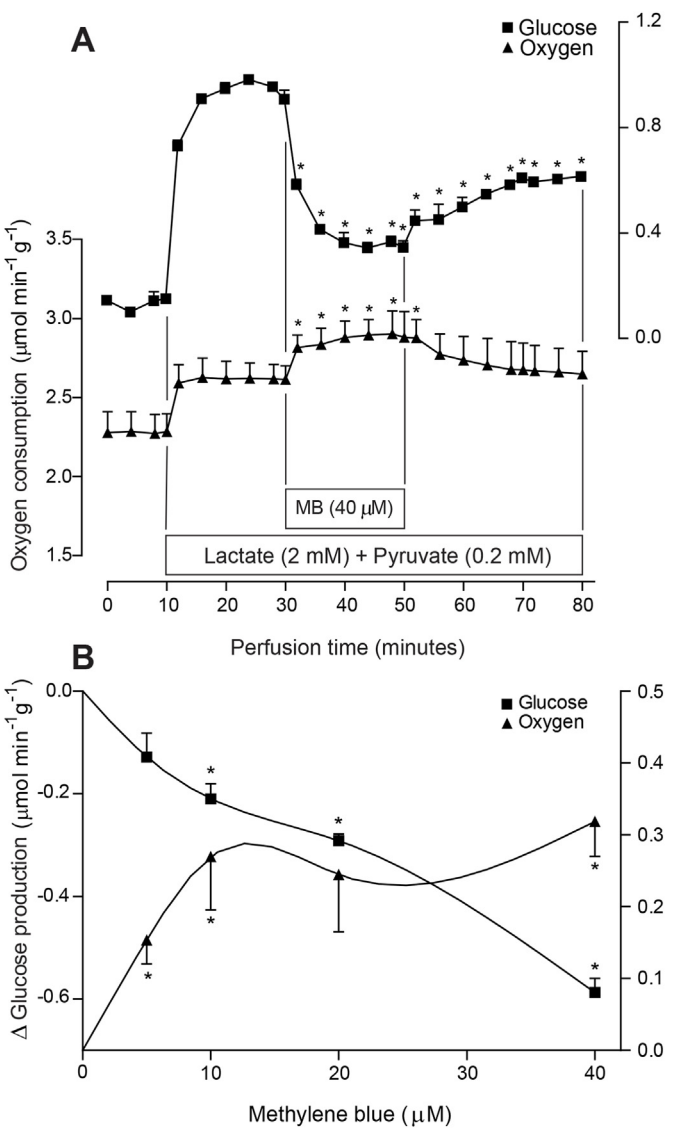

Fig. 10. The effects of methylene blue (MB) on the metabolic fluxes from lactate and pyruvate in perfused livers isolated from fasted rats. Livers from 12 h fasted rats were perfused as described in the Materials and Methods section. Panel A: time courses of the changes caused by 40 μM methylene blue for glucose production and oxygen consumption. Lactate and pyruvate were infused at 10–80 min and methylene blue was infused at 30–50 min, as indicated by the horizontal bars. Panel B: concentration-dependent effects of methylene blue on glucose production and oxygen consumption. These effects were determined as the difference between the rates in the presence of lactate plus pyruvate alone and the maximal (or minimal) rates after the onset of methylene blue infusion. Each experimental point is the mean ± standard error of the mean of 3–4 experiments. Asterisks indicate a statistical significance in comparison with the control condition as revealed by Student's *t*-test ($p < 0.05$).

3.16. The direct effects of MB on oxygen consumption by perfused livers and microsomal electron transport

Fig. 13A shows that potassium cyanide infusion in perfused livers caused an extensive reduction of respiration (from 1.86 ± 0.15 to 0.72 ± 0.07 μmol/min^{-1} × g^{-1}). The latter denotes the microsomal oxygen consumption and the loss of oxygen by diffusion during a single passage through the liver. Under this condition the infusion of 40 μM MB increased the oxygen consumption.

The effects of MB on the microsomal electron transport were examined by incubating isolated microsomes with NADPH (Fig. 13B). Adding NADPH started an electron transfer to oxygen without extra

Table 2
The effects of methylene blue on hepatic adenine nucleotide contents in substrate-perfused livers of fasted rats. Livers from fasted rats were perfused in an open system as described in the Materials and Methods section. Lactate (2.0 mM) and pyruvate (0.2 mM) were infused at 10 min, and 40 μM methylene blue was infused 20 min after the beginning of the lactate and pyruvate infusion. The livers were freeze-clamped in liquid nitrogen and extracted with perchloric acid. The neutralized extracts were used for adenine nucleotide determination by HPLC. Control determinations were performed with livers that were freeze-clamped at the same perfusion time but without methylene blue infusion.

Condition	ATP	ADP	AMP	AMP + ADP + ATP	ATP/ADP ratio	ATP/AMP ratio
	μmol × (g liver weight)$^{-1}$					
Control (n = 7)	1.53 ± 0.13	0.52 ± 0.04	0.38 ± 0.08	2.41 ± 0.14	2.98 ± 0.39	5.69 ± 1.46
Methylene blue (40 μM) (n = 4)	1.42 ± 0.15	0.77 ± 0.05*	0.64 ± 0.09*	2.17 ± 0.16	1.82 ± 0.11*	2.32 ± 0.42

Values are means ± standard errors of the means.
Significantly different from the corresponding control values according to Student's *t*-test ($p < 0.05$).

additions and the succeeding addition of MB produced a clear stimulation in oxygen consumption. Numerical interpolation revealed 50% stimulation at the MB concentration of 22.58 μM.

4. Discussion

The main conclusion that can be drawn from this study is that MB can interact with mitochondria, and, when photoactivated, it is capable of damaging specific structures and molecules even at low oxygen concentration condition, compromising mitochondrial energy metabolism. However, without photoactivation, MB also interacts with mitochondrial structures and negatively interferes in mitochondrial respiration, acting predominantly as an uncoupler of oxidative phosphorylation. Consequently, MB is also able to perturb the liver metabolism, altering several metabolic pathways related to energy metabolism.

The relatively hydrophobic nature of MB [55] seems to be one of the most important factors for its interaction with cellular structures, as indicated by experimental and molecular dynamic experiments [56,57]. This feature probably promotes extensive interaction with mitochondrial membranes and proteins, as further demonstrated experimentally in this study with or without the influence of light. Although the exact binding sites of MB to mitochondria were not identified, some general considerations regarding the interaction of MB with mitochondrial lipids can be drawn from the binding curves reproduced with isolated mitochondria using the analysis of Salla and colleagues [32]. For the concentration of 40 μM MB, the use of linear regression coefficients between 0.3189 and 0.3736 generates values between 12.75 nmol and 14.94 nmol bound MB per mg protein. As in adult fed rats, the protein/phospholipid ratio is approximately 4.6 [58], this would correspond to 60.69—68.72 nmol MB per mg phospholipid. Assuming an average phospholipid molecular mass of 750 g/mol [59], this would correspond to molar MB/phospholipid ratios between 0.0455 and 0.0515. This means that MB corresponded to 4.55%—5.15%

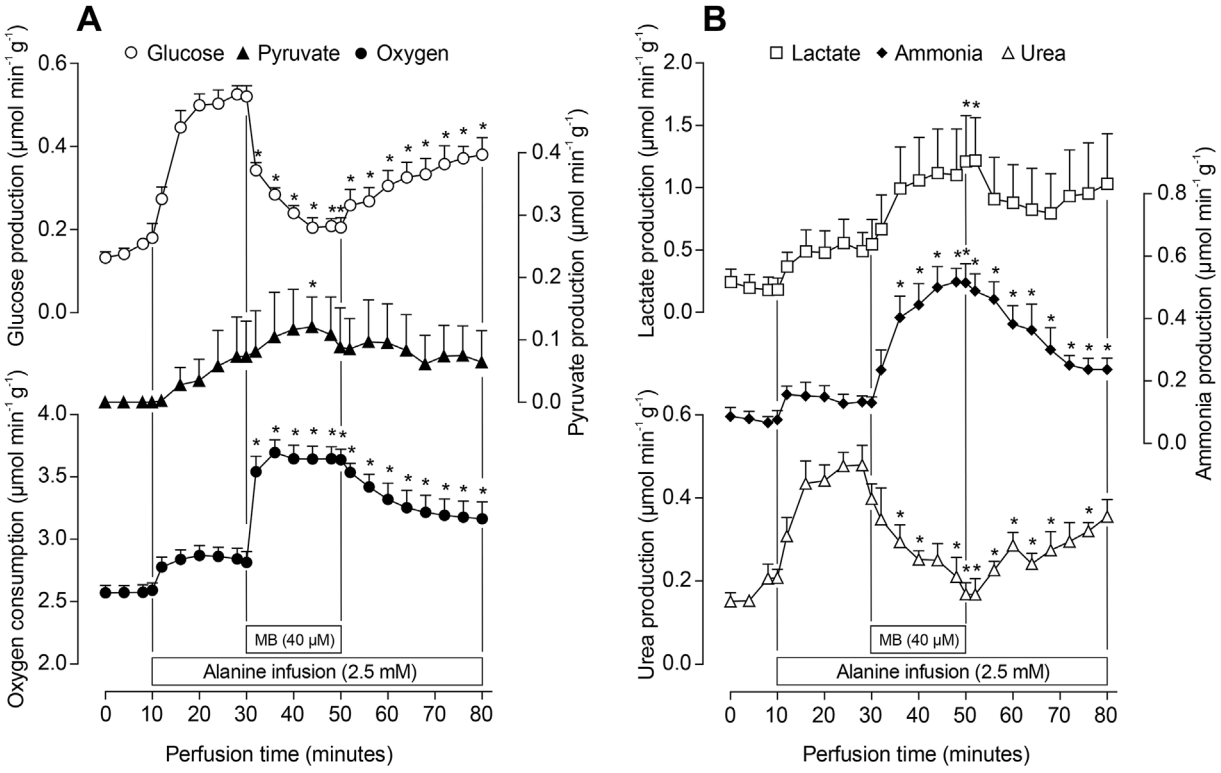

Fig. 11. Time courses of the effects of 40 μM methylene blue (MB) on glucose and pyruvate production and oxygen consumption (A) as well as lactate, urea and ammonia production (B) derived from alanine in perfused livers from 12 h fasted rats. Livers from 12 h fasted rats were perfused as described in the Materials and Methods section. Alanine was infused at 10–80 min and methylene blue was infused at 30–50 min, as indicated by the horizontal bars. Each experimental point is the mean ± standard error of the mean of 5 experiments. Asterisks indicate a statistical significance in comparison with the control condition (values obtained immediately before methylene blue infusion) as revealed by Student's *t*-test ($p < 0.05$).

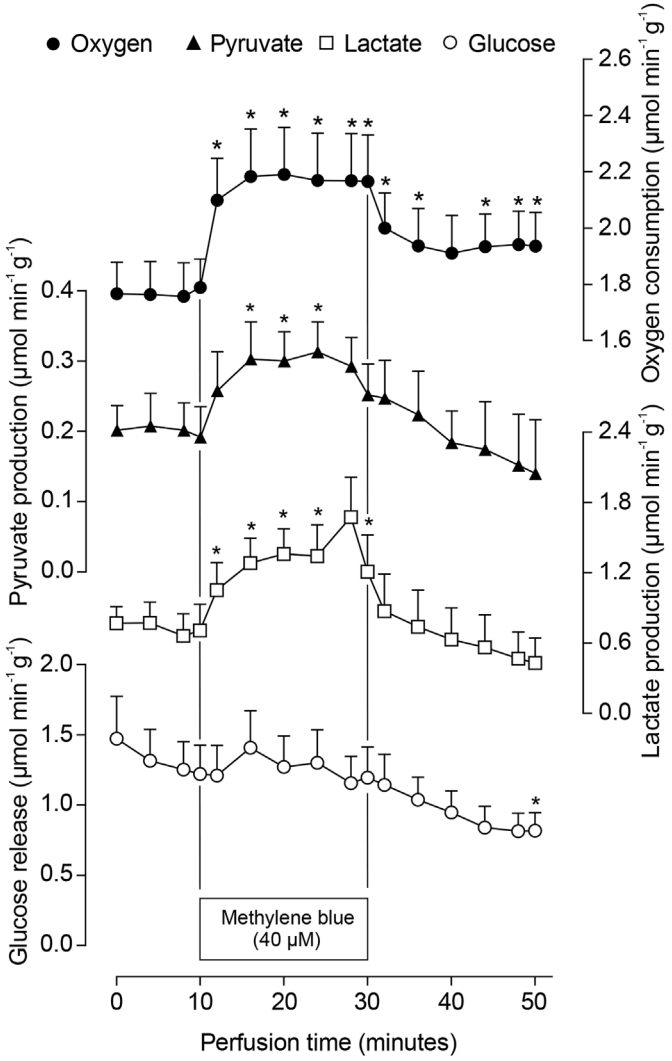

Fig. 12. Time courses of the changes caused by 40 μM methylene blue in glycogen catabolism and oxygen uptake. Livers from fed rats were perfused as described in the Materials and Methods section using substrate-free perfusion medium. Methylene blue was infused at 10–30 min, as indicated by the horizontal bar. Each experimental point is the mean ± standard error of the mean of 5 experiments. Asterisks indicate a statistical significance in comparison with the control condition (values obtained immediately before methylene blue infusion) as revealed by Student's *t*-test ($p < 0.05$).

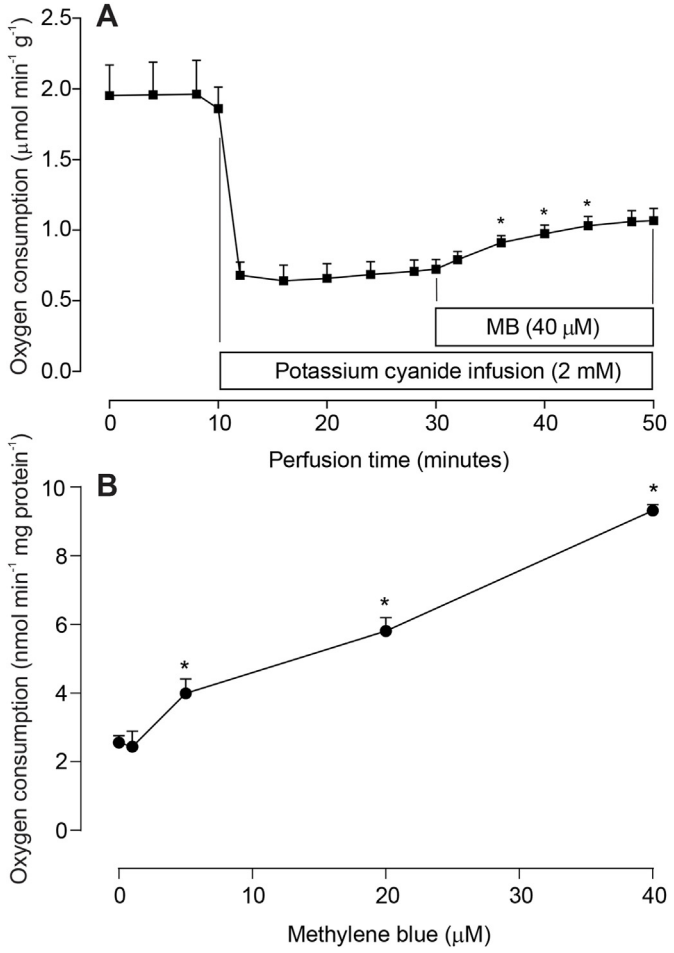

Fig. 13. Panel A: changes in hepatic oxygen consumption caused by 40 μM methylene blue with respiratory chain blockage with 2 mM cyanide. Livers were perfused in an open system as described in the Materials and Methods section using substrate-free perfusion medium. Panel B: the effects of methylene blue on microsomal respiration driven by NADPH. Microsomes were isolated and incubated at 37 °C in reaction medium as described in the Materials and Methods section. Oxygen consumption began with the addition of 1 mM NADPH, which was followed by the addition of methylene blue (1, 5, 20 or 40 μM, as indicated). Oxygen consumption rates were evaluated in the absence (basal rates) or presence of methylene blue and were computed from the slopes of the recorder tracings. Asterisks indicate a statistical significance in comparison with the control condition as revealed by Student's *t*-test (A) or ANOVA with post hoc Dunnett's test (B) ($p < 0.05$).

of the total phospholipids in the mitochondrial membranes, a finding that is in accordance with the lack of saturation of MB binding. In our incubation system, neither mitochondrial energization nor photostimulation influenced MB interaction with mitochondria. Paradoxically, a possible explanation for the lack of efficacy of the $\Delta\Psi_m$ in inducing MB accumulation lies in the fact that this drug is positively charged. As a cationic PS, MB may induce mitochondrial depolarization and consequently restrict its own accumulation into the mitochondrial matrix [3]. The dissipation of the mitochondrial proton gradient by MB corroborates previous observations [16] and is in line with our finding that MB acted as an uncoupler of oxidative phosphorylation even without photostimulation. Such behaviour reinforces the suggestion that the accumulation of cationic PSs in the mitochondria depends on other factors, such as their degree of lipophilicity, in addition to the charge for proper targeting [60].

The experiments with DCFH allowed us to examine in detail the ability of MB to generate oxidizing species after 10 min of light exposure in an environment analogous to that of pathological hypoxia (oxygen level of 3.68 mmHg or 190 μM), a condition predominantly found in solid tumours [25]. Even in this condition, under photostimulation in a mitochondria-free system MB was able to generate expressive amounts of oxidizing species, as indicated by DCF fluorescence [33,61]. This effect is in line with the fact that, as a Type II PS, MB is an efficient $^1O_2$ generator [3,7]. However, under the influence of light, besides $^1O_2$ generation, MB takes part in reactions that can generate other transient species [42,62], including its semireduced ($MB^{\bullet}$) and dication ($MB^{2+\bullet}$) radicals. The former can be oxidized by molecular oxygen returning to the ground-state MB and forming $O_2^{\bullet-}$, another potentially cytotoxic compound [63]. Considering that several one-electron-oxidizing species can oxidize DCFH to DCF [64], the DCF fluorescence could be a result not only of the reaction of $^1O_2$ with DCFH [61] but also of $MB^{\bullet}$, $MB^{2+\bullet}$ and $O_2^{\bullet-}$ radicals. A surprising finding was the MB capacity to generate oxidizing species without the influence of light. Although no mechanistic characterization for this effect can be drawn from our experimental data, it is known that some compounds chemically convert DCFH to the DCF fluorescent moiety without the

participation of free radicals [65]. This seems to be the case for MB.

Even knowing that the environment in which a PS is located has a strong influence on its photochemical reactions [3,7], the results of DCF experiments indicated that if MB was bound to mitochondria under the influence of light, the organelle would experience a high oxidative stress, with possible damage to its structures. The obtained results under MB photostimulation were coherent with an environment under considerable oxidative stress, as can be concluded from the increased lipid peroxidation and protein carbonylation. It seems plausible to highlight the role of $^1O_2$ in these findings as the reaction of $^1O_2$ with membrane lipids results in lipid peroxidation and can lead to disruption of cellular membranes [2,66,67]. It is also possible that the reaction of $^1O_2$ with aromatic residues of amino acids, such as tryptophan, may be responsible for at least part of the observed higher levels of protein carbonyl groups found under MB photostimulation [2,68]. Other important sources of protein carbonyl groups include the lipid peroxidation products, such as malonaldehyde and 4-hydroxynonenal, which readily attack nucleophilic groups in proteins, provoking irreversible damage of vital proteins [69]. Although MB is recognized as a highly efficient Type II PS [3], one cannot exclude the possibility that the mitochondrial oxidative damage can alternatively be caused by Type I reactions. The latter reactions often involve the initial production of superoxide ($O_2^{\bullet-}$) either through the oxidation of the semireduced form of MB ($MB^{\bullet}$) or electron transfer from the triplet-excited MB to molecular oxygen [1,63]. The $O_2^{\bullet-}$ ultimately leads to the formation of other ROS, such as H_2O_2 and the highly reactive and dangerous $HO^{\bullet}$ [1,2]. Due the high reactivity and short half-life of $^1O_2$ and $HO^{\bullet}$, only mitochondrial molecules and structures that are next to the region of their synthesis (sites of MB interaction) could be affected by these ROS [1,2]. These characteristics suggest that both mitochondrial lipids and proteins may interact intimately with MB, representing potential targets for the direct and photodynamic effects of this compound.

The results of this study indicate that the non-enzymatic ROS-scavenging system of mitochondria is impaired by MB when the compound is photoactivated. As we have found, the mitochondrial pool of reduced GSH was significantly reduced in response to MB photostimulation. Although it is challenging to define the precise cause of this effect, it could be attributed at least partially to GSH-based antioxidant mechanisms in which ROS are scavenged by the enzyme glutathione peroxidase (GPx), which requires GSH as an electron donor. Considering that this protective mechanism is habitually activated under high oxidative stress conditions, depletion of GSH is an expected phenomenon [70]. An alternative explanation is the ability of photostimulated MB to directly decrease the GSH contents, as demonstrated in the current study. This effect is probably caused by the non-enzymatic reaction of GSH with oxidizing species, such as $O_2^{\bullet-}$, $HO^{\bullet}$, 4-hydroxynonenal, or other transient species of MB produced when the compound is photostimulated [71–73]. The possibility of a direct conjugation reaction between MB and GSH is improbable [74], because no effect of MB without light influence was detected on GSH levels *in vitro*. As some studies demonstrated that the high GSH levels of neoplastic cells could compromise the efficacy of PDT [74,75], depleting mitochondrial GSH by MB's photodynamic effects could boost the efficacy of this PS. Contrary to previous arguments for other PSs [76], the oxidation of mitochondrial protein thiol groups seems not to be an important mechanism of MB's photodynamic effects. As we have found, the total content of protein thiols in mitochondria was not significantly altered by MB either in the dark or under light. Contrasting to responses found under MB photostimulation, MB did not show any clear ability to induce oxidative stress in mitochondria, as can be deduced from the markers of oxidative injury (TBARS and carbonylated proteins) and redox buffers (GSH and protein thiols) measured in the present study. Under photostimulation, however, the injuries to mitochondrial lipids and proteins produced by MB at low levels of oxygen seem to be the consequence of an induction of both a pro-oxidant environment and a deficient antioxidant defence system.

Considering the phototoxic damage caused by MB in mitochondria, it is not surprising that the mitochondrial respiration can also be affected, thereby compromising ATP production. In fact, the results of the present study confirmed the findings of Visarius and colleagues [16] with regards to the uncoupling action of MB. MB stimulated oxygen consumption in the absence of exogenous ADP (substrate and state IV respiration), inhibited oxygen consumption in the presence of exogenous ADP (state III respiration), decreased the RC ratio, and decreased the ADP/O ratio, a pattern of events that commonly occurs in the presence of an uncoupler of oxidative phosphorylation [32,77]. The effects on the ATPase activity give additional evidence of an uncoupling effect. MB stimulated the ATPase activity in intact and coupled mitochondria, but when the ATPase was already stimulated by 2,4-dinitrophenol or by freeze-thaw disruption of the mitochondria, MB was no longer effective. It is well known that the ATPase activity in intact and coupled mitochondria is retroactively limited by the electrochemical proton gradient generated by proton extrusion. Any compound that promotes a dissipation of this gradient will cause stimulation of the ATPase activity, along with a stimulation of respiratory activity in intact mitochondria. It is noteworthy that such effects were caused by relatively low concentrations of MB. When succinate was used as the substrate, for example, substrate and state IV respiration were stimulated by 93.6% and 93.9% in the presence of 5 μM and 2 μM MB, respectively. Thus, the effects caused by MB are comparable to those of the classical uncoupler 2,4-dinitrophenol, which stimulates half-maximally oxygen uptake in isolated mitochondria within the range of 15–20 μM [32,78]. Mechanistically, MB could uncouple the oxidative phosphorylation in different ways. As a cationic PS, MB could dissipate the $\Delta\Psi_m$ by its transfer into the mitochondrial matrix across the inner mitochondrial membrane. MB could also act as a protonophore, passively transporting protons down the mitochondrial electrochemical gradient [79]. This is corroborated by the fact that the chemical structure of MB bears essential general features that can be expected for protonophore uncouplers: a lipophilic central structure with protonatable groups [55]. Such compounds typically interact and bind very effectively to mitochondrial membranes [56,57]. Because the protonation of the central ring nitrogen is favoured at low pH [80], the acidic environment near to the intermembrane space may favour the protonophore effect of MB. Additionally, as MB possesses an affinity for the lipidic phase of the biological membranes [55–57], the uncoupling effect might be due to an increase in permeability caused by a direct interaction of MB with the inner mitochondrial membrane. This interpretation is in accordance with the fact that MB stimulates the NADH oxidation by intact mitochondria in the dark, reproducing the observations of Visarius and colleagues [16]. A stimulus in the basal NADH oxidation would be apparent only if the inner mitochondrial membrane was damaged. In combination or separately, these three possible mechanisms of the uncoupling action of MB are corroborated by the inhibition of mitochondrial swelling generated by both electron transport and ATP hydrolysis. As swelling in the presence of acetate as a permeant ion depends on the establishment of proton electrochemical gradient across inner mitochondrial membrane, any compound that dissipates this gradient will promote inhibition of mitochondrial swelling [48].

An additional effect for MB in a specific site of the electron transport chain was suggested by several observations: a more prominent inhibition on state III respiration when succinate (FAD-dependent) was the electron donor in comparison with malate and glutamate (NAD^+-dependent); the inhibition on succinate-oxidase activity but not on NADH-oxidase activity or oxidation of TMPD-ascorbate; a higher decrease of the swelling amplitude of mitochondrial swelling driven by succinate oxidation than those driven by glutamate, TMPD-ascorbate or ATP. Although the exact site of this action cannot be inferred from the data, MB could be acting in a specific segment preceding the transfer of the electrons from complex II to complex III. If so, inhibition of dehydrogenation reaction of succinate is improbable because MB did not

alter succinate dehydrogenase activity in the dark. It should be commented that this inhibition in a specific segment of the respiratory chain did not limit mitochondrial respiration under conditions in which the rate of oxygen consumption is controlled by the proton electrochemical gradient, considering that both basal respiration and state IV driven by succinate oxidation were not inhibited, but, on the contrary, stimulated by MB. Another question that can be raised is the stimulus of NADH oxidase activity by MB in disrupted mitochondria, a process that could also affect the oxidative phosphorylation. This effect reproduced the observations of Sevcík and Dunford [43], revealing that NADH directly and non-enzymatically reduces MB under light or dark conditions, which in turn can be reoxidized by molecular oxygen even in the absence of suitable electron acceptors, such as cytochrome *c* [81]. In addition, MB can be efficiently reduced by several NAD(P)H-dependent dehydrogenases (e.g. NADH-dehydrogenase of complex I) [17,81]. Besides the stimulus on NADH oxidase, the possibility that the non-enzymatic reactions could be responsible for part of the oxygen consumption stimulus in intact mitochondria when NAD^+-dependent substrates were used as electron donors cannot be excluded. As proven, the combination of these multiple and complex effects exerted by MB on mitochondria led to a severe impairment of the ATP production capacity in the dark.

As is clear from the discussed results, MB by itself inhibits the mitochondrial energy metabolism by at least two mechanisms: (a) the uncoupling of oxidative phosphorylation; and (b) the inhibition of the electron transfer chain. Upon photostimulation, however, these effects were much stronger, and MB was deleterious to mitochondria at relatively low concentrations. As can be deduced from the values of RC ratios and ADP/O ratios shown in Table 1, under the influence of light, the maximal uncoupling effect is reached at 1 μM MB, whereas at least 10 μM (with succinate) and 40 μM (with glutamate plus malate) are required to reach an equivalent degree of uncoupling in the dark. This difference can be explained by two factors. The first and simplest explanation is that the elevated oxidizing species production upon MB photostimulation can promote lipid peroxidation, which may, in turn, lead to inner mitochondrial membrane damage, proton leak, and, consequently, uncoupling of oxidative phosphorylation. The second factor to this enhanced uncoupling effect is the onset of the mitochondrial permeability transition, a phenomenon which is induced under oxidative stress condition [82]. As an expected initial consequence of the permeability transition pore opening, mitochondria uncouple and undergo respiration functional injury [82]. Both interpretations agree with the fact that – although to a lesser degree – MB potentiates the NADH oxidation by intact mitochondria even upon photostimulation, denoting changes in the integrity of the inner mitochondrial membrane. If one considers the absolute values presented in Fig. 8E, it is clear that the maximal value in the presence of light is smaller than the value in its absence. This is probably due to the fact that – besides causing mitochondrial inner membrane injury – MB also leads to photodynamic inactivation of components of the mitochondrial respiratory machinery. Indeed, an expressive photoinactivation of complex II is indicated by the inhibition of succinate oxidase and succinate dehydrogenase activities. A slight influence on complex I is also suggested by the significant inhibition of NADH oxidase activity at low MB concentrations. Apparently, the photoinactivation of specific complexes of the respiratory chain in intact-coupled mitochondria was more drastic than in disrupted mitochondria as can be deduced from the lack of stimulatory effect of MB on substrate and state IV respiration, an effect that was found in the dark condition. Probably, the uncoupler action of MB was overlapped by photoinactivation of the mitochondrial electron transport chain. Direct photoinactivation of the F_1F_O–ATP synthase complex is also probable as indicated by the finding that upon photostimulation, MB inhibits the ATPase activity of disrupted and uncoupled mitochondria. The tendency of increase on ATPase activity of intact-coupled mitochondria by MB in the range up to 5 μM, followed by the suppression of this effect at higher MB concentrations, seems also to be the consequence of the photoinactivation effect superimposing the uncoupling effect.

As oxidizing species, such as $^1O_2$ and $HO^{\bullet}$, have short lifespans [1,2], it can be speculated that the F_1F_O–ATP synthase complex, complex II, and, to a lesser degree, complex I may interact intimately with MB, representing specific mitochondrial targets for the photodynamic effects of this compound. However, the fact that photoinactivation of cytochrome *c* oxidase (complex IV) was negligible when MB was applied at concentrations up to 40 μM is a sign that the photodynamic effects of MB do not cause indiscriminate damage and are rather selective, with different proteins exhibiting clearly different sensitivities. Moreover, it cannot be excluded that the photoinactivation of some proteins is at least partially caused by secondary products of photoinduced lipid peroxidation and reactive products resulting from decomposition of protein peroxides [83]. It has been also shown that photoinactivation of proteins of the electron transport chain provokes a burst of ROS production [84], which in turn could cause additional damage of different mitochondrial structures. It seems plausible that these mechanisms are involved in the inhibition of the mitochondrial respiration in intact-coupled mitochondria which was found only under MB photostimulation.

The results found in the perfused rat liver clearly revealed that the effects of MB observed in isolated mitochondria were clearly manifested in intact livers, being compatible with its uncoupling effect. The direct indicators of the impairment of mitochondrial function in the intact liver were the stimulation of oxygen consumption in the livers of fed and fasted animals and the change in the ATP/ADP ratio in the livers of fasted animals. Consistently, MB was able to inhibit gluconeogenesis and ureogenesis (ammonia detoxification), two biosynthetic routes dependent on energy in the form of ATP. For lactate, pyruvate, and alanine gluconeogenesis, pyruvate carboxylase is known as the rate-limiting enzyme, as can be presumed from its flux control coefficient (between 56% and 75%) [85]. The rate-limiting step in the urea cycle is catalysed by the enzyme carbamoyl-phosphate synthetase 1, with a flux control coefficient of above 90% [86,87]. Thus, a decrease in cellular ATP levels would lead to an inhibition of gluconeogenesis and ureogenesis by inhibiting these reactions, which are dependent on ATP. Besides inhibition of gluconeogenesis, the inhibition of pyruvate carboxylation is also probably responsibly for the observed increments in pyruvate and lactate outputs when alanine was used as the gluconeogenic substrate.

Alternatively, the MB biotransformation could also be contributing to these metabolic disturbances. As demonstrated here and elsewhere [43], MB has been shown to be a pro-oxidative agent, that is, it was able to non-enzymatically oxidize NADH *in vitro*. It has been suggested that this reaction may also occur *in vivo* in the intact cells [7]. In this case, a competition for NADH could occur between the respiratory chain and MB, which anticipate NADH oxidation. In this condition, if the reduced form of MB does not directly reduce cytochrome *c*, as stated above [17,81], this may contribute to a reduction in the formation of mitochondrial ATP and, consequently, inhibit biosynthetic pathways. This effect would be relevant for gluconeogenesis inhibition, which in addition to being dependent on mitochondrial ATP formation, requires reducing power of NADH at the glyceraldehyde 3-phosphate dehydrogenase step. The possibility that these reactions could be responsible for part of the oxygen consumption stimulus and gluconeogenesis inhibition in the intact liver cannot be excluded. Additionally, according to Medscape [88], MB is metabolized by different isoforms of the cytochrome P450 (CYP450) system and UDP-glucuronosyltransferases (UGTs). The MB biotransformation includes, for example, N-demethylation reactions [26,89]. These reactions may indeed occur in the microsomal electron transport system (CYP450) and require NADPH as a source of electron. In this sense, the diversion of a fraction of glucose 6-phosphate or malate for the synthesis of NADPH is a likely phenomenon, because, apparently, microsomal electron transport (CYP450) stimulation by MB was found to occur in both the perfused liver and

isolated microsomes. Such deviations would lead to an inhibition of gluconeogenesis. Accordingly, conjugation of MB metabolites to glucuronic acid catalysed by UGTs are equally possible. Within the liver, the main source of glucuronic acid is normally glycogenolysis, but in the virtual absence of glycogen, gluconeogenesis is the sole possible source [54,90,91]. Therefore, it is quite possible that the diversion of a fraction of the glucose 6-phospate for glucuronidation reactions is another factor that may be contributing to gluconeogenesis inhibition.

MB was also able to activate glycogenolysis and glycolysis in the livers of fed animals. It is well known that the levels of adenine nucleotides are also modulators of glycogenolysis and glycolysis. Thus, stimulation of glycolysis is an expected compensatory phenomenon for decreased mitochondrial ATP formation and increased NADH oxidation, whereas stimulation of glycogenolysis is a means of providing glucose 6-phosphate for the increased glycolytic flux [32,77]. A question that can be raised at this point regards the lack of stimulation of glucose output from glycogen, an observation that contradicts both the stimulation of glycogenolysis and glycolysis state above. With the data currently available, the diversion of a fraction of glucose 6-phosphate for the synthesis of NADPH and glucuronidation reactions is the only explanation for this contradictory effect. This phenomenon would result not only in the inhibition of gluconeogenesis, but also in a significant diminution in the rate of glucose output from the liver of fed rats.

A question that merits further discussion is whether the dark toxic effects of MB demonstrated in isolated mitochondria and perfused liver could have implications for *in vivo* physiological condition. The MB concentrations employed here were mainly based on recently published data reporting the photodynamic effects of this compound [9,24,92]. However, other relevant aspects were also taken into consideration. Clinically, MB is administered intravenously or orally, and the dose depends on the therapeutic indication. To give some examples, for the treatment of ifosfamid-induced neurotoxicity, the recommended dose of MB is 3—6 × 50 mg/day orally or intravenously. For inherited methemoglobinemia, the suggested oral dose is 1 × 50—250 mg/day (for a lifetime). In particular circumstances, as in a controlled trial study conducted on semi-immune patients with uncomplicated falciparum malaria, the oral dose was 2 × 390 mg/day [11,93,94]. Although it is not always easy to associate doses to systemic concentrations and the latter to tissue concentrations, some considerations can be made. MB is well absorbed from the gastrointestinal tract, such that peak plasma concentrations are reached 2 h after oral administration [14,95]. According to a study performed using a sample of healthy volunteers, a mean peak plasma concentration of 5 μM MB is achieved after an intravenous bolus injection of 100 mg [96]. In another study conducted using a sample of healthy volunteers, the dose of 500 mg led to peak concentrations of MB in plasma of up to 21 μM [95]. Here, the MB concentration producing half-maximal rates of inhibition of gluconeogenesis from lactate and pyruvate was 20.2 μM, an effect comparable to that of the classical uncoupler 2,4-dinitrophenol, which inhibits half-maximally alanine gluconeogenesis at the concentration of 17.9 μM [32,77]. Considering all these points, as well as the central role of the liver in xenobiotic metabolism and the fact that the portal concentration can achieve levels much higher than in the systemic circulation [97,98], we cannot exclude the possibility that effects like those reported here can be significant for the liver under physiological conditions, especially if high doses of MB are ingested or injected. Therefore, the metabolic impairments revealed in this study could contribute to adverse effects in patients during MB administration. As for other inhibitors of oxidative phosphorylation [32,77,99], one can expect glucose homeostasis perturbations due to gluconeogenesis inhibition and glycogenolysis stimulation, metabolic acidosis due the reduced rate of conversion of lactate and pyruvate into glucose and to excess lactate production from glycolysis, and the impairment of ammonia detoxification. Indeed, acidosis is one of a series of acute toxic effects that have been described in animals exposed to MB [100]. Since several of MB's effects observed in this study are certainly of mitochondrial origin, and the mitochondria from any tissue can provide energy in the form of ATP, it is highly probable that the effects are not restricted to the liver. In rats, for example, 60 min after oral administration or intravenous injection, MB concentrations are around 10 times higher in the brain than in plasma [101], making this organ particularly susceptible to energy impairments.

In conclusion, the results of the present study corroborate recent findings of other studies that MB has potential for use in PDT [9,24,92,102,103]. In this sense, MB has the physicochemical and photodynamic features necessary to interact with mitochondria and, upon photostimulation, oxidatively damage lipids and proteins even under low oxygen concentrations, severely compromising ATP biosynthesis. The impairment of mitochondrial bioenergetics jointly with exaggerated oxidizing species production such as ROS may lead to several disturbances in metabolite and macromolecule synthesis, active transport systems, membrane integrity, and others. This combination can be particularly effective against cancer cells, because besides being more vulnerable to oxidative stress, they also need energy in the form of ATP for proliferation, invasion, and metastasis [104,105]. This is also in line with the fact that excessive ROS production and massive ATP depletion in mitochondria are involved in the specific mechanisms that lead to cell death [106]. Probably due to its hydrophilic/hydrophobic balance, MB is one of those compounds that is distributed in several cellular compartments – including, besides mitochondria, lysosomes. This multiplicity of intracellular targets should not necessarily be considered negative within PDT, as it may represent an efficient pathway to induce cell death [107]. Contrary to what is expected for an ideal PS [2], MB has been shown to be toxic even in the absence of irradiation, substantially inhibiting the mitochondrial energy metabolism and causing energy-linked liver metabolic changes. Its actions on intact liver and isolated mitochondria are comparable despite the different conditions of both experimental systems. Paradoxically, the MB concentration range employed in the present study is similar to the concentration ranges for which various beneficial effects have been attributed to the compound, such as optimizing brain metabolism, increasing oxidative phosphorylation, and restoring mitochondrial electron transport in situations of drug-induced toxicity [17–19,108]. Despite the findings presented, further experimental and clinical investigations are necessary to validate the potential use of MB in mitochondria-targeted PDT and to clarify if the undesirable effects reported here can really occur *in vivo*. If so, to increase the MB selectivity towards cancer cells, direct application of the drug into the affected zone or even the use of metal-MB nanoparticles and MB-encapsulated liposomes for targeted cancer cells could be valuable strategies to minimize side effects [92,109].

Funding

This study was supported by grants from the National Council for Scientific and Technological Development (CNPq), Araucaria Foundation (FA) and Coordination for the Improvement of Higher Education Personnel (CAPES). The sponsors had no involvement in the study design; the execution of research; the interpretation of findings; the writing of the report or in the decision to submit the article for publication.

Declaration of competing interest

The authors declare that they have no known competing financial interests or personal relationships that could have appeared to influence the work reported in this paper.

Acknowledgments

The authors would like to express their gratitude for the technical

assistance of Aparecida Pinto Munhos Hermoso and Célia Akemi Gasparetto. We also gratefully acknowledge the instrumental research facilities provided by the Complexo de Centrais de Apoio à Pesquisa (COMCAP) at the State University of Maringá (UEM).

References

[1] A.P. Castano, T.N. Demidova, M.R. Hamblin, Mechanisms in photodynamic therapy: part one-photosensitizers, photochemistry and cellular localization, Photodiagnosis Photodyn. Ther. 1 (4) (2004) 279–293, https://doi.org/10.1016/S1572-1000(05)00007-4.

[2] D. van Straten, V. Mashayekhi, H.S. de Bruijn, S. Oliveira, D.J. Robinson, Oncologic photodynamic therapy: basic principles, current clinical status and future directions, Cancers 9 (2) (2017) 1–54, https://doi.org/10.3390/cancers9020019.

[3] C.S. Oliveira, R. Turchiello, A.J. Kowaltowski, G.L. Indig, M.S. Baptista, Major determinants of photoinduced cell death: subcellular localization versus photosensitization efficiency, Free Radic. Biol. Med. 51 (4) (2011) 824–833, https://doi.org/10.1016/j.freeradbiomed.2011.05.023.

[4] L. Huang, T.G. St Denis, Y. Xuan, Y.Y. Huang, M. Tanaka, A. Zadlo, T. Sarna, M.R. Hamblin, Paradoxical potentiation of methylene blue-mediated antimicrobial photodynamic inactivation by sodium azide: role of ambient oxygen and azide radicals, Free Radic. Biol. Med. 53 (11) (2012) 2062–2071, https://doi.org/10.1016/j.freeradbiomed.2012.09.006.

[5] J. Zhang, C. Jiang, J.P. Figueiro Longo, R.B. Azevedo, H. Zhang, L.A. Muehlmann, An updated overview on the development of new photosensitizers for anticancer photodynamic therapy, Acta Pharm. Sin. B 8 (2) (2018) 137–146, https://doi.org/10.1016/j.apsb.2017.09.003.

[6] L.Z. Zhang, G.Q. Tang, The binding properties of photosensitizer methylene blue to herring sperm DNA: a spectroscopic study, J. Photochem. Photobiol., B 74 (2–3) (2004) 119–125, https://doi.org/10.1016/j.jphotobiol.2004.03.005.

[7] J.P. Tardivo, A. Del Giglio, C.S. de Oliveira, D.S. Gabrielli, H.C. Junqueira, D.B. Tada, D. Severino, R. de Fatima Turchiello, M.S. Baptista, Methylene blue in photodynamic therapy: from basic mechanisms to clinical applications, Photodiagnosis Photodyn. Ther. 2 (3) (2005) 175–191, https://doi.org/10.1016/S1572-1000(05)00097-9.

[8] D.Y. Seong, Y.J. Kim, Enhanced photodynamic therapy efficacy of methylene blue-loaded calcium phosphate nanoparticles, J. Photochem. Photobiol., B 146 (2015) 34–43, https://doi.org/10.1016/j.jphotobiol.2015.02.022.

[9] A.F. Dos Santos, L.F. Terra, R.A. Wailemann, T.C. Oliveira, V.M. Gomes, M.F. Mineiro, F.C. Meotti, A. Bruni-Cardoso, M.S. Baptista, L. Labriola, Methylene blue photodynamic therapy induces selective and massive cell death in human breast cancer cells, BMC Canc. 17 (1) (2017) 194, https://doi.org/10.1186/s12885-017-3179-7.

[10] J. Vara, M.S. Gualdesi, V. Aiassa, C.S. Ortiz, Evaluation of physicochemical properties and bacterial photoinactivation of phenothiazine photosensitizers, Photochem. Photobiol. Sci. 18 (6) (2019) 1576–1586, https://doi.org/10.1039/c8pp00584b.

[11] R.H. Schirmer, H. Adler, M. Pickhardt, E. Mandelkow, Lest we forget you - methylene blue…, Neurobiol. Aging 32 (12) (2011), https://doi.org/10.1016/j.neurobiolaging.2010.12.012 2325.e7-2325.e16.

[12] L. Tretter, G. Horvath, A. Holgyesi, F. Essek, V. Adam-Vizi, Enhanced hydrogen peroxide generation accompanies the beneficial bioenergetic effects of methylene blue in isolated brain mitochondria, Free Radic. Biol. Med. 77 (2014) 317–330, https://doi.org/10.1016/j.freeradbiomed.2014.09.024.

[13] P. Haouzi, M. Gueguinou, T. Sonobe, A. Judenherc-Haouzi, N. Tubbs, M. Trebak, J. Cheung, F. Bouillaud, Revisiting the physiological effects of methylene blue as a treatment of cyanide intoxication, Clin. Toxicol. 56 (9) (2018) 828–840, https://doi.org/10.1080/15563650.2018.1429615.

[14] G. Lu, M. Nagbanshi, N. Goldau, M. Mendes Jorge, P. Meissner, A. Jahn, F.P. Mockenhaupt, O. Muller, Efficacy and safety of methylene blue in the treatment of malaria: a systematic review, BMC Med. 16 (1) (2018) 59, https://doi.org/10.1186/s12916-018-1045-3.

[15] S. Piel, J.K. Ehinger, I. Chamkha, E.Å. Frostner, F. Sjövall, E. Elmér, M.J. Hansson, Bioenergetic bypass using cell-permeable succinate, but not methylene blue, attenuates metformin-induced lactate production, Intensive Care Med. Exp. 6 (1) (2018) 1–12, https://doi.org/10.1186/s40635-018-0186-1.

[16] T.M. Visarius, J.W. Stucki, B.H. Lauterburg, Stimulation of respiration by methylene blue in rat liver mitochondria, FEBS Lett. 412 (1) (1997) 157–160, https://doi.org/10.1016/s0014-5793(97)00767-9.

[17] K.K. Lee, U.A. Boelsterli, Bypassing the compromised mitochondrial electron transport with methylene blue alleviates efavirenz/isoniazid-induced oxidant stress and mitochondria-mediated cell death in mouse hepatocytes, Redox Biol. 2 (2014) 599–609, https://doi.org/10.1016/j.redox.2014.03.003.

[18] G.R. Choudhury, A. Winters, R.M. Rich, M.G. Ryou, Z. Gryczynski, F. Yuan, S.H. Yang, R. Liu, Methylene blue protects astrocytes against glucose oxygen deprivation by improving cellular respiration, PloS One 10 (4) (2015) 1–14, https://doi.org/10.1371/journal.pone.0123096.

[19] K.K. Lee, N. Imaizumi, S.R. Chamberland, N.N. Alder, U.A. Boelsterli, Targeting mitochondria with methylene blue protects mice against acetaminophen-induced liver injury, Hepatology 61 (1) (2015) 326–336, https://doi.org/10.1002/hep.27385.

[20] D. Tucker, Y. Lu, Q. Zhang, From mitochondrial function to neuroprotection—an emerging role for methylene blue, Mol. Neurobiol. 55 (6) (2018) 5137–5153, https://doi.org/10.1007/s12035-017-0712-2.

[21] H. Atamna, A. Nguyen, C. Schultz, K. Boyle, J. Newberry, H. Kato, B.N. Ames, Methylene blue delays cellular senescence and enhances key mitochondrial biochemical pathways, Faseb. J. 22 (3) (2008) 703–712, https://doi.org/10.1096/fj.07-9610com.

[22] H. Atamna, R. Kumar, Protective role of methylene blue in Alzheimer's disease via mitochondria and cytochrome c oxidase, J. Alzheimers Dis. 20 (s2) (2010) S439–S452, https://doi.org/10.3233/JAD-2010-100414.

[23] E.J. Lim, C.H. Oak, J. Heo, Y.H. Kim, Methylene blue-mediated photodynamic therapy enhances apoptosis in lung cancer cells, Oncol. Rep. 30 (2) (2013) 856–862, https://doi.org/10.3892/or.2013.2494.

[24] B. Kofler, A. Romani, C. Pritz, T.B. Steinbichler, V.H. Schartinger, H. Riechelmann, J. Dudas, Photodynamic effect of methylene blue and low level laser radiation in head and neck squamous cell carcinoma cell lines, Int. J. Mol. Sci. 19 (4) (2018) 1–17, https://doi.org/10.3390/ijms19041107.

[25] S.R. McKeown, Defining normoxia, physoxia and hypoxia in tumours—implications for treatment response, Br. J. Radiol. 87 (1035) (2014) 1–12, https://doi.org/10.1259/bjr.20130676.

[26] A. Warth, B. Goeppert, C. Bopp, P. Schirmacher, C. Flechtenmacher, J. Burhenne, Turquoise to dark green organs at autopsy, Virchows Arch. 454 (3) (2009) 341–344, https://doi.org/10.1007/s00428-009-0734-x.

[27] P.R. Ryle, J. Chakraborty, A.D. Thomson, The effect of methylene blue on the hepatocellular redox state and liver lipid content during chronic ethanol feeding in the rat, Biochem. J. 232 (3) (1985) 877–882, https://doi.org/10.1042/bj2320877.

[28] R. Scholz, T. Bücher, Hemoglobin-free perfusion of rat liver, in: B. Chance, R.W. Estabrook, J.R. Williamson (Eds.), Control of Energy Metabolism, Academic Press, New York, 1965, pp. 393–414.

[29] D.O. Voss, A.P. Campello, M. Bacila, The respiratory chain and the oxidative phosphorylation of rat brain mitochondria, Biochem. Biophys. Res. Commun. 4 (1961) 48–51, https://doi.org/10.1016/0006-291x(61)90253-4.

[30] A. Bracht, E.L. Ishii-Iwamoto, A.M. Kelmer-Bracht, O Estudo do Metabolismo no Fígado em Perfusão, in: A. Bracht, E.L. Ishii-Iwamoto (Eds.), Métodos de Laboratório em Bioquímica, Sao Paulo, Manole, 2003, pp. 275–289.

[31] O.H. Lowry, N.J. Rosebrough, A.L. Farr, R.J. Randall, Protein measurement with the Folin phenol reagent, J. Biol. Chem. 193 (1) (1951) 265–275.

[32] G.B.F. Salla, L. Bracht, A.B. de Sa-Nakanishi, A.V. Parizotto, F. Bracht, R.M. Peralta, A. Bracht, Distribution, lipid-bilayer affinity and kinetics of the metabolic effects of dinoseb in the liver, Toxicol. Appl. Pharmacol. 329 (2017) 259–271, https://doi.org/10.1016/j.taap.2017.06.013.

[33] A.S. Garcez, S.C. Nunez, M.S. Baptista, N.A. Daghastanli, R. Itri, M.R. Hamblin, M.S. Ribeiro, Antimicrobial mechanisms behind photodynamic effect in the presence of hydrogen peroxide, Photochem. Photobiol. Sci. 10 (4) (2011) 483–490, https://doi.org/10.1039/c0pp00082e.

[34] F.A. Guarnier, A.L. Cecchini, A.A. Suzukawa, A.L. Maragno, A.N. Simao, M.D. Gomes, R. Cecchini, Time course of skeletal muscle loss and oxidative stress in rats with Walker 256 solid tumor, Muscle Nerve 42 (6) (2010) 950–958, https://doi.org/10.1002/mus.21798.

[35] H. Ohkawa, N. Ohishi, K. Yagi, Assay for lipid peroxides in animal tissues by thiobarbituric acid reaction, Anal. Biochem. 95 (2) (1979) 351–358, https://doi.org/10.1016/0003-2697(79)90738-3.

[36] J. Sedlak, R.H. Lindsay, Estimation of total, protein-bound, and nonprotein sulfhydryl groups in tissue with Ellman's reagent, Anal. Biochem. 25 (1) (1968) 192–205, https://doi.org/10.1016/0003-2697(68)90092-4.

[37] P.J. Hissin, R. Hilf, A fluorometric method for determination of oxidized and reduced glutathione in tissues, Anal. Biochem. 74 (1) (1976) 214–226, https://doi.org/10.1016/0003-2697(76)90326-2.

[38] L.C. Clark Jr., Monitor and control of blood and tissue oxygen tensions, Am. Soc. Artif. Intern. Organs J. 2 (1) (1956) 41–48.

[39] B. Chance, G.R. Williams, The respiratory chain and oxidative phosphorylation, Adv. Enzymol. Relat. Subj. Biochem. 17 (1956) 65–134, https://doi.org/10.1002/9780470122624.ch2.

[40] T.P. Singer, Determination of the activity of succinate, NADH, choline, and alpha-glycerophosphate dehydrogenases, Methods Biochem. Anal. 22 (1974) 123–175, https://doi.org/10.1002/9780470110423.ch3.

[41] C.P. Colturato, R.P. Constantin, A.S. Maeda Jr., R.P. Constantin, N.S. Yamamoto, A. Bracht, E.L. Ishii-Iwamoto, J. Constantin, Metabolic effects of silibinin in the rat liver, Chem. Biol. Interact. 195 (2) (2012) 119–132, https://doi.org/10.1016/j.cbi.2011.11.006.

[42] D. Gabrielli, E. Belisle, D. Severino, A.J. Kowaltowski, M.S. Baptista, Binding, aggregation and photochemical properties of methylene blue in mitochondrial suspensions, Photochem. Photobiol. 79 (3) (2004) 227–232, https://doi.org/10.1562/be-03-27.1.

[43] P. Sevcík, H.B. Dunford, Kinetics of the oxidation of NADH by methylene blue in a closed system, J. Phys. Chem. 95 (6) (1991) 2411–2415, https://doi.org/10.1021/j100159a054.

[44] M.E. Pullman, H.S. Penefsky, A. Datta, E. Racker, Partial resolution of the enzymes catalyzing oxidative phosphorylation. I. Purification and properties of soluble dinitrophenol-stimulated adenosine triphosphatase, J. Biol. Chem. 235 (11) (1960) 3322–3329.

[45] C.H. Fiske, Y. Subarrow, The colorimetric determination of phosphorus, J. Biol. Chem. 66 (2) (1925) 375–400.

[46] A. Bracht, E.L. Ishii-Iwamoto, C.L. Salgueiro-Pagadigorria, O estudo do metabolismo energético em mitocôndrias isoladas de tecido animal, in: A. Bracht, E.L. Ishii-Iwamoto (Eds.), Métodos de laboratório em bioquímica, Manole, São Paulo, 2003, pp. 227–248.

[47] I.R. Lanza, K.S. Nair, Functional assessment of isolated mitochondria in vitro,

Methods Enzymol. 457 (2009) 349–372, https://doi.org/10.1016/S0076-6879(09)05020-4.
[48] M.G. Mustafa, K. Utsumi, L. Packer, Damped oscillatory control of mitochondrial respiration and volume, Biochem. Biophys. Res. Commun. 24 (3) (1966) 381–385, https://doi.org/10.1016/0006-291x(66)90168-9.
[49] G.L. Ellman, Tissue sulfhydryl groups, Arch. Biochem. Biophys. 82 (1) (1959) 70–77, https://doi.org/10.1016/0003-9861(59)90090-6.
[50] H.U. Bergmeyer, Methods of Enzymatic Analysis, 2nd English ed., Academic Press, New York, 1974.
[51] N. Shimojo, K. Naka, C. Nakajima, C. Yoshikawa, K. Okuda, K. Okada, Test-strip method for measuring lactate in whole blood, Clin. Chem. 35 (9) (1989) 1992–1994.
[52] K. Mihara, R. Sato, Partial purification of NADH-cytochrome b5 reductase from rabbit liver microsomes with detergents and its properties, J. Biochem. 71 (4) (1972) 725–735.
[53] H. de Groot, T. Noll, H. Sies, Oxygen dependence and subcellular partitioning of hepatic menadione-mediated oxygen uptake. Studies with isolated hepatocytes, mitochondria, and microsomes from rat liver in an oxystat system, Arch. Biochem. Biophys. 243 (2) (1985) 556–562, https://doi.org/10.1016/0003-9861(85)90532-6.
[54] G.J. Eler, R.M. Peralta, A. Bracht, The action of n-propyl gallate on gluconeogenesis and oxygen uptake in the rat liver, Chem. Biol. Interact. 181 (3) (2009) 390–399, https://doi.org/10.1016/j.cbi.2009.07.006.
[55] S. Selvam, I. Sarkar, Bile salt induced solubilization of methylene blue: study on methylene blue fluorescence properties and molecular mechanics calculation, J. Pharm. Anal. 7 (1) (2017) 71–75, https://doi.org/10.1016/j.jpha.2016.07.006.
[56] T.F. Schmidt, L. Caseli, O.N. Oliveira, R. Itri, Binding of methylene blue onto Langmuir monolayers representing cell membranes may explain its efficiency as photosensitizer in photodynamic therapy, Langmuir 31 (14) (2015) 4205–4212, https://doi.org/10.1021/acs.langmuir.5b00166.
[57] N.I. Ercan, P. Stroeve, J.W. Tringe, R. Faller, Molecular dynamics modeling of methylene blue− DOPC lipid bilayer interactions, Langmuir 34 (14) (2018) 4314–4323, https://doi.org/10.1021/acs.langmuir.8b00372.
[58] J.K. Pollak, E.A. Munn, The isolation by isopycnic density-gradient centrifugation of two mitochondrial populations from livers of embryonic and fed and starved adult rats, Biochem. J. 117 (5) (1970) 913–919, https://doi.org/10.1042/bj1170913.
[59] M.E. Sommer, W.C. Smith, D.L. Farrens, Dynamics of arrestin-rhodopsin interactions: acidic phospholipids enable binding of arrestin to purified rhodopsin in detergent, J. Biol. Chem. 281 (14) (2006) 9407–9417, https://doi.org/10.1074/jbc.M510037200.
[60] J. Morgan, A.R. Oseroff, Mitochondria-based photodynamic anti-cancer therapy, Adv. Drug Deliv. Rev. 49 (1–2) (2001) 71–86, https://doi.org/10.1016/s0169-409x(01)00126-0.
[61] N.A. Daghastanli, R. Itri, M.S. Baptista, Singlet oxygen reacts with 2',7'-dichlorodihydrofluorescein and contributes to the formation of 2',7'-dichlorofluorescein, Photochem. Photobiol. 84 (5) (2008) 1238–1243, https://doi.org/10.1111/j.1751-1097.2008.00345.x.
[62] D. Severino, H.C. Junqueira, M. Gugliotti, D.S. Gabrielli, M.S. Baptista, Influence of negatively charged interfaces on the ground and excited state properties of methylene blue, Photochem. Photobiol. 77 (5) (2003) 459–468, https://doi.org/10.1562/0031-8655(2003)077<0459:ioncio>2.0.co;2.
[63] M. Hayyan, M.A. Hashim, I.M. AlNashef, Superoxide ion: generation and chemical implications, Chem. Rev. 116 (5) (2016) 3029–3085, https://doi.org/10.1021/acs.chemrev.5b00407.
[64] B. Kalyanaraman, V. Darley-Usmar, K.J. Davies, P.A. Dennery, H.J. Forman, M.B. Grisham, G.E. Mann, K. Moore, L.J. Roberts 2nd, H. Ischiropoulos, Measuring reactive oxygen and nitrogen species with fluorescent probes: challenges and limitations, Free Radic. Biol. Med. 52 (1) (2012) 1–6, https://doi.org/10.1016/j.freeradbiomed.2011.09.030.
[65] L.M. Tetz, P.W. Kamau, A.A. Cheng, J.D. Meeker, R. Loch-Caruso, Troubleshooting the dichlorofluorescein assay to avoid artifacts in measurement of toxicant-stimulated cellular production of reactive oxidant species, J. Pharmacol. Toxicol. Methods 67 (2) (2013) 56–60, https://doi.org/10.1016/j.vascn.2013.01.195.
[66] T.A. Dix, J. Aikens, Mechanisms and biological relevance of lipid peroxidation initiation, Chem. Res. Toxicol. 6 (1) (1993) 2–18, https://doi.org/10.1021/tx00031a001.
[67] S.P. Stratton, D.C. Liebler, Determination of singlet oxygen-specific versus radical-mediated lipid peroxidation in photosensitized oxidation of lipid bilayers: effect of beta-carotene and alpha-tocopherol, Biochemistry 36 (42) (1997) 12911–12920, https://doi.org/10.1021/bi9708646.
[68] J.A. Silvester, G.S. Timmins, M.J. Davies, Protein hydroperoxides and carbonyl groups generated by porphyrin-induced photo-oxidation of bovine serum albumin, Arch. Biochem. Biophys. 350 (2) (1998) 249–258, https://doi.org/10.1006/abbi.1997.0495.
[69] M. Fedorova, R.C. Bollineni, R. Hoffmann, Protein carbonylation as a major hallmark of oxidative damage: update of analytical strategies, Mass Spectrom. Rev. 33 (2) (2014) 79–97, https://doi.org/10.1002/mas.21381.
[70] H.M. Lee, C.W. Chung, C.H. Kim, D.H. Kim, T.W. Kwak, Y.I. Jeong, D.H. Kang, Defensive mechanism in cholangiocarcinoma cells against oxidative stress induced by chlorin e6-based photodynamic therapy, Drug Des. Dev. Ther. 8 (2014) 1451–1462, https://doi.org/10.2147/DDDT.S62265.
[71] M.A. Keller, G. Piedrafita, M. Ralser, The widespread role of non-enzymatic reactions in cellular metabolism, Curr. Opin. Biotechnol. 34 (2015) 153–161, https://doi.org/10.1016/j.copbio.2014.12.020.
[72] P. Patlevič, J. Vašková, P. Švorc, L. Vaško, P. Švorc, Reactive oxygen species and antioxidant defense in human gastrointestinal diseases, Integrative Med. Res. 5 (4) (2016) 250–258, https://doi.org/10.1016/j.imr.2016.07.004.
[73] S. Kwiecien, K. Jasnos, M. Magierowski, Z. Sliwowski, R. Pajdo, B. Brzozowski, T. Mach, D. Wojcik, T. Brzozowski, Lipid peroxidation, reactive oxygen species and antioxidative factors in the pathogenesis of gastric mucosal lesions and mechanism of protection against oxidative stress - induced gastric injury, J. Physiol. Pharmacol. 65 (5) (2014) 613–622.
[74] T.A. Theodossiou, C.E. Olsen, M. Jonsson, A. Kubin, J.S. Hothersall, K. Berg, The diverse roles of glutathione-associated cell resistance against hypericin photodynamic therapy, Redox Biol. 12 (2017) 191–197, https://doi.org/10.1016/j.redox.2017.02.018.
[75] H. Hu, J. Chen, H. Yang, X. Huang, H. Wu, Y. Wu, F. Li, Y. Yi, C. Xiao, Y. Li, Y. Tang, Z. Li, B. Zhang, X. Yang, Potentiating photodynamic therapy of ICG-loaded nanoparticles by depleting GSH with PEITC, Nanoscale 11 (13) (2019) 6384–6393, https://doi.org/10.1039/c9nr01306g.
[76] P.A. Tsaytler, M. C O'Flaherty, D.V. Sakharov, J. Krijgsveld, M.R. Egmond, Immediate protein targets of photodynamic treatment in carcinoma cells, J. Proteome Res. 7 (9) (2008) 3868–3878, https://doi.org/10.1021/pr800189q.
[77] S.C. Saling, J.F. Comar, M.S. Mito, R.M. Peralta, A. Bracht, Actions of juglone on energy metabolism in the rat liver, Toxicol. Appl. Pharmacol. 257 (3) (2011) 319–327, https://doi.org/10.1016/j.taap.2011.09.004.
[78] J.B. Chappell, The effects of 2,4-dinitrophenol on mitochondrial oxidations, Biochem. J. 90 (2) (1964), https://doi.org/10.1042/bj0900237 237-237.
[79] S.G. McLaughlin, J.P. Dilger, Transport of protons across membranes by weak acids, Physiol. Rev. 60 (3) (1980) 825–863, https://doi.org/10.1152/physrev.1980.60.3.825.
[80] J. Chen, T.C. Cesario, P.M. Rentzepis, Effect of pH on methylene blue transient states and kinetics and bacteria photoinactivation, J. Phys. Chem. 115 (13) (2011) 2702–2707, https://doi.org/10.1021/jp110215g.
[81] H. Atamna, J. Mackey, J.M. Dhahbi, Mitochondrial pharmacology: electron transport chain bypass as strategies to treat mitochondrial dysfunction, Biofactors 38 (2) (2012) 158–166, https://doi.org/10.1002/biof.197.
[82] S. Qi, L. Guo, S. Yan, R.J. Lee, S. Yu, S. Chen, Hypocrellin A-based photodynamic action induces apoptosis in A549 cells through ROS-mediated mitochondrial signaling pathway, Acta Pharm. Sin. B 9 (2) (2019) 279–293, https://doi.org/10.1016/j.apsb.2018.12.004.
[83] A.M. Odeh, J.D. Craik, R. Ezzeddine, A. Tovmasyan, I. Batinic-Haberle, L.T. Benov, Targeting mitochondria by Zn (II) N-alkylpyridylporphyrins: the impact of compound sub-mitochondrial partition on cell respiration and overall photodynamic efficacy, PloS One 9 (9) (2014), https://doi.org/10.1371/journal.pone.0108238 e108238-e108238.
[84] S. Wu, F. Zhou, Y. Wei, W.R. Chen, Q. Chen, D. Xing, Cancer phototherapy via selective photoinactivation of respiratory chain oxidase to trigger a fatal superoxide anion burst, Antioxidants Redox Signal. 20 (5) (2014) 733–746, https://doi.org/10.1089/ars.2013.5229.
[85] A.K. Groen, C.W. van Roermund, R.C. Vervoorn, J.M. Tager, Control of gluconeogenesis in rat liver cells. Flux control coefficients of the enzymes in the gluconeogenic pathway in the absence and presence of glucagon, Biochem. J. 237 (2) (1986) 379–389, https://doi.org/10.1042/bj2370379.
[86] A.J. Meijer, Insensitivity of carbamoyl-phosphate synthetase towards inhibition by carbamoyl phosphate makes it unlikely that mitochondrial metabolite transport controls ornithine cycle flux, in: A. Azzi, K.A. Nałęz, M.J. Nałęcz, L. Wojtczak (Eds.), Anion Carriers of Mitochondrial Membranes, Springer, Berlin, 1989, pp. 307–315.
[87] M.L. Summar, J.V. Gainer, M. Pretorius, H. Malave, S. Harris, L.D. Hall, A. Weisberg, D.E. Vaughan, B.W. Christman, N.J. Brown, Relationship between carbamoyl-phosphate synthetase genotype and systemic vascular function, Hypertension 43 (2) (2004) 186–191, https://doi.org/10.1161/01.HYP.0000112424.06921.52.
[88] Medscape, Provayblue (methylene blue) dosing, indications, interactions, adverse effects, and more, https://reference.medscape.com/drug/provayblue-methylene-blue-343739, (2020) , Accessed date: 27 March 2020.
[89] A. Petzer, B.H. Harvey, G. Wegener, J.P. Petzer, B. Azure, A metabolite of methylene blue, is a high-potency, reversible inhibitor of monoamine oxidase, Toxicol. Appl. Pharmacol. 258 (3) (2012) 403–409, https://doi.org/10.1016/j.taap.2011.12.005.
[90] R. Scholz, W. Hansen, R.G. Thurman, Interaction of mixed-function oxidation with biosynthetic processes. 1. Inhibition of gluconeogenesis by aminopyrine in perfused rat liver, Eur. J. Biochem. 38 (1) (1973) 64–72, https://doi.org/10.1111/j.1432-1033.1973.tb03034.x.
[91] G. Bánhegyi, T. Garzó, F. Antoni, J. Mandl, Glycogenolysis-and not gluconeogenesis-is the source of UDP-glucuronic acid for glucuronidation, Biochim. Biophys. Acta Gen. Subj. 967 (3) (1988) 429–435, https://doi.org/10.1016/0304-4165(88)90106-7.
[92] P.T. Wu, C.L. Lin, C.W. Lin, N.C. Chang, W.B. Tsai, J. Yu, Methylene-blue-encapsulated liposomes as photodynamic therapy nano agents for breast cancer cells, Nanomaterials 9 (1) (2019), https://doi.org/10.3390/nano9010014 14-14.
[93] J. Pelgrims, F. De Vos, J. Van den Brande, D. Schrijvers, A. Prove, J.B. Vermorken, Methylene blue in the treatment and prevention of ifosfamide-induced encephalopathy: report of 12 cases and a review of the literature, Br. J. Canc. 82 (2) (2000) 291–294, https://doi.org/10.1054/bjoc.1999.0917.
[94] M. Bountogo, A. Zoungrana, B. Coulibaly, C. Klose, U. Mansmann, F.P. Mockenhaupt, J. Burhenne, G. Mikus, I. Walter-Sack, R.H. Schirmer, A. Sie, P. Meissner, O. Muller, Efficacy of methylene blue monotherapy in semi-immune adults with uncomplicated falciparum malaria: a controlled trial in Burkina Faso, Trop. Med. Int. Health 15 (6) (2010) 713–717, https://doi.org/10.1111/j.1365-

3156.2010.02526.x.
[95] I. Walter-Sack, J. Rengelshausen, H. Oberwittler, J. Burhenne, O. Mueller, P. Meissner, G. Mikus, High absolute bioavailability of methylene blue given as an aqueous oral formulation, Eur. J. Clin. Pharmacol. 65 (2) (2009) 179–189, https://doi.org/10.1007/s00228-008-0563-x.
[96] C. Aeschlimann, T. Cerny, A. Kupfer, Inhibition of (mono)amine oxidase activity and prevention of ifosfamide encephalopathy by methylene blue, Drug Metab. Dispos. 24 (12) (1996) 1336–1339.
[97] D.J. Hoffman, T. Seifert, A. Borre, H.N. Nellans, Method to estimate the rate and extent of intestinal absorption in conscious rats using an absorption probe and portal blood sampling, Pharmaceut. Res. 12 (6) (1995) 889–894, https://doi.org/10.1023/a:1016221322886.
[98] K. Yamano, K. Yamamoto, M. Katashima, H. Kotaki, S. Takedomi, H. Matsuo, H. Ohtani, Y. Sawada, T. Iga, Prediction of midazolam—cyp3a inhibitors interaction in the human liver from in vivo/in vitro absorption, distribution, and metabolism data, Drug Metabol. Dispos. 29 (4) (2001) 443–452.
[99] V.O. Pateis, L. Bracht, L.S. Castro, G.B.F. Salla, J.F. Comar, A.V. Parizotto, R.M. Peralta, A. Bracht, The food additive BHA modifies energy metabolism in the perfused rat liver, Toxicol. Lett. 299 (2018) 191–200, https://doi.org/10.1016/j.toxlet.2018.10.005.
[100] S.S. Auerbach, D.W. Bristol, J.C. Peckham, G.S. Travlos, C.D. Hebert, R.S. Chhabra, Toxicity and carcinogenicity studies of methylene blue trihydrate in F344N rats and B6C3F1 mice, Food Chem. Toxicol. 48 (1) (2010) 169–177, https://doi.org/10.1016/j.fct.2009.09.034.
[101] C. Peter, D. Hongwan, A. Kupfer, B.H. Lauterburg, Pharmacokinetics and organ distribution of intravenous and oral methylene blue, Eur. J. Clin. Pharmacol. 56 (3) (2000) 247–250, https://doi.org/10.1007/s002280000124.
[102] V.P.S. Jesus, L. Raniero, G.M. Lemes, T.T. Bhattacharjee, P.C. Caetano Junior, M.L. Castilho, Nanoparticles of methylene blue enhance photodynamic therapy, Photodiagnosis Photodyn. Ther. 23 (2018) 212–217, https://doi.org/10.1016/j.pdpdt.2018.06.011.
[103] A.P. Silva, C.L. Neves, E.D.A. Silva, T.C.L. Portela, R.S. Iunes, B. Cogliati, D. Severino, M.D.S. Baptista, M.L.Z. Dagli, F.J.H. Blazquez, J. Silva, Effects of methylene blue-mediated photodynamic therapy on a mouse model of squamous cell carcinoma and normal skin, Photodiagnosis Photodyn. Ther. 23 (2018) 154–164, https://doi.org/10.1016/j.pdpdt.2018.06.012.
[104] J. Verrax, N. Dejeans, B. Sid, C. Glorieux, P.B. Calderon, Intracellular ATP levels determine cell death fate of cancer cells exposed to both standard and redox chemotherapeutic agents, Biochem. Pharmacol. 82 (11) (2011) 1540–1548, https://doi.org/10.1016/j.bcp.2011.07.102.
[105] F. Lin, Y.W. Bao, F.G. Wu, Improving the phototherapeutic efficiencies of molecular and nanoscale materials by targeting mitochondria, Molecules 23 (11) (2018) 1–23, https://doi.org/10.3390/molecules23113016.
[106] Y. Yang, G. Jiang, P. Zhang, J. Fan, Programmed cell death and its role in inflammation, Mil Med. Res. 2 (1) (2015) 12, https://doi.org/10.1186/s40779-015-0039-0.
[107] W.K. Martins, N.F. Santos, C.d.S. Rocha, I.O.L. Bacellar, T.M. Tsubone, A.C. Viotto, A.Y. Matsukuma, A.B.d.P. Abrantes, P. Siani, L.G. Dias, M.S. Baptista, Parallel damage in mitochondria and lysosomes is an efficient way to photoinduce cell death, Autophagy 15 (2) (2019) 259–279, https://doi.org/10.1080/15548627.2018.1515609.
[108] A.L. Lin, E. Poteet, F. Du, R.C. Gourav, R. Liu, Y. Wen, A. Bresnen, S. Huang, P.T. Fox, S.H. Yang, T.Q. Duong, Methylene blue as a cerebral metabolic and hemodynamic enhancer, PloS One 7 (10) (2012) 1–9, https://doi.org/10.1371/journal.pone.0046585.
[109] J. Yu, C.H. Hsu, C.C. Huang, P.Y. Chang, Development of therapeutic Au-methylene blue nanoparticles for targeted photodynamic therapy of cervical cancer cells, ACS Appl. Mater. Interfaces 7 (1) (2015) 432–441, https://doi.org/10.1021/am5064298.